

MESTRADO

MEDICINA E ONCOLOGIA MOLECULAR

von Willebrand Factor as a Biomarker of Aortic Stenosis Severity

Ana Rita Nunes Albuquerque

M

2021



FACULDADE DE MEDICINA



MESTRADO

MEDICINA E ONCOLOGIA MOLECULAR

von Willebrand Factor as a Biomarker of Aortic Stenosis Severity

Ana Rita Nunes Albuquerque

Supervisor:

Doctor Isabel Miranda

Department of Surgery and Physiology, Faculty of Medicine, University of Porto

Co-supervisors:

Doctor Fábio Trindade

Department of Surgery and Physiology, Faculty of Medicine, University of Porto

Carla Sousa, MD

Department of Cardiology, Hospital Center of São João (CHUSJ), Porto

Department of Surgery and Physiology, Faculty of Medicine, University of Porto





AGRADECIMENTOS

O trabalho desenvolvido nesta tese não seria possível sem a ajuda dos meus orientadores, aos quais agradeço a toda a orientação prestada, motivação e disponibilidade ao longo deste ano.

Estendo o meu agradecimento também a todas as pessoas do departamento de fisiologia que de forma direta, ou indireta, contribuíram para elaboração da tese.

Não podia deixar de agradecer a minha família, em especial, aos meus pais aos quais agradeço todo o encorajamento, carinho e paciência. Sem vocês não teria sido possível. Um especial agradecimento também ao meu irmão e cunhada pela companhia, disponibilidade, e pelos inúmeros desvaneios.

Aos meus amigos, que na grande maior parte, mesmo permanecendo à distância estiveram sempre disponíveis para o que fosse necessário. Agradeço todo o apoio e motivação assim como todas as conversas intermináveis, videochamadas, sessões de estudo e desabafos.

A todos, os meus sinceros agradecimentos.





TABLE OF CONTENTS

Abstract.....	ii
Resumo.....	iv
List of figures.....	vi
Supplementary Figures	viii
List of tables	ix
supplementary tables	x
List of abbreviations	xi
Definitions	xiv
Preamble.....	xvi
Introduction	1
<i>Calcific Aortic Valve Disease: Epidemiology and Risk Factors</i>	2
<i>Pathophysiology of CAVD</i>	2
<i>Management and Treatment of CAVD</i>	4
Why is surgery/intervention the only option?.....	4
Diagnosis and classification of AVS	5
TAVI versus SAVR.....	7
<i>von Willebrand Disease: History, epidemiology, and disease subtypes</i>	7
<i>Treatment of vWD</i>	8
<i>Acquired von Willebrand Syndrome</i>	11
<i>Diagnostic tests for vWD and AvWS</i>	12
<i>von Willebrand Factor: The molecular basics</i>	15
<i>von Willebrand Factor: an important regulator of hemostasis</i>	16
<i>Less Known roles of vWF</i>	18
<i>Aims</i>	20
Materials and methods	21
<i>Sample collection and ethics statement</i>	22
<i>Platelet-poor plasma protocol optimization</i>	22
<i>vWF relative quantification through Slot Blot analysis</i>	23
<i>vWF absolute quantification through ELISA</i>	24

<i>Assessment of the vWF multimer profile by Immuno-Electrophoresis</i>	25
<i>Analysis of the vWF multimer pattern</i>	26
<i>Statistical Analysis</i>	26
Results	28
<i>Optimization of the protocol to obtain platelet-poor plasma</i>	29
<i>vWF relative quantification through Slot Blot analysis</i>	33
<i>vWF multimer profile analysis after normalization via absolute quantification</i>	36
<i>Can vWF the multimer profile be a biomarker for AVS?</i>	38
Baseline population characteristics	38
Correlation of the vWF multimeric profile with parameters of disease severity before and after aortic valve replacement.....	40
Differences in vWF HMWM loss before and after aortic valve replacement	44
Discussion	45
Conclusions	51
Supplements	53

ABSTRACT

Aortic valve stenosis (AVS) is the most common valve disease, and its incidence is only expected to rise with an ever-increasing older population. The only available treatment option encompasses aortic valve replacement (AVR), which can be performed by open heart surgery, or by transcatheter aortic valve implantation (TAVI).

Both approaches carry the risk of paravalvular regurgitation, although TAVI is associated with a higher risk. Echocardiography remains the gold standard for the assessment of AVS severity as well as paravalvular regurgitation severity, but the latter, in particular, can be challenging to appraise only by this imaging technique. In this regard, circulating biomarkers may provide helpful insight into disease severity and into AVR complications.

von Willebrand factor (vWF) is a circulating multimeric glycoprotein involved in primary and secondary hemostasis. vWF multimers are present in the plasma in a wide range of sizes; however, with turbulent blood flow, associated with AVS, and with paravalvular regurgitation, the multimers are fragmented, leading to an abnormal decrease of higher molecular weight vWF multimers (HMWM). The HMWM are the most biologically active, hence their loss leads to impaired coagulation, and to an increased risk of bleeding. Changes in the multimer profile can be monitored by immunoelectrophoresis. After aortic valve replacement, in the absence of regurgitation or after its successful correction, the vWF recovers its normal multimeric pattern.

In this sense, the vWF multimer pattern was studied on a cohort of patients previously submitted to surgical AVR with the goal of evaluating the vWF multimer pattern in patients with AVS before and after intervention, and its usefulness as a biomarker of AVS severity. The cohort included 30 patients, of which, 13 had both pre- and postoperative blood collections.

In this thesis, the vWF multimer pattern was evaluated with three different methods. Method 1 was based in the peak intensities of the vWF multimers profile. Method 2 consisted of counting vWF multimers. Lastly, in method 3, the retardation factor was used as a measure of HMWM loss. Additionally, the index of the HMWM of the patients divided by that of a control sample was also calculated for all the methods used. All these techniques to assess the vWF multimer pattern were then correlated with echocardiography parameters used to evaluate the severity of AVS.

Focusing exclusively on preoperative samples (N=30), we found correlations between the vWF multimer pattern and the AVS parameters, namely with the mean and maximal transvalvular pressure gradient. Using method 2 and its index, no correlations were found

between the vWF multimer profile and parameters of AVS severity. vWF profile correlated with the mean transvalvular pressure gradient, when applying methods 1 and 3, along with method 1 index ($r=-0.359$, $p=0.051$; $r=-0.564$, $p=0.001$; $r=-0.409$, $p=0.02$ respectively). Furthermore, the analysis carried out by method 1 index and method 3 showed a correlation between the vWF profile and the maximum gradient ($r=-0.428$ $p=0.03$; $r=-0.572$, $p=0.002$; respectively). No correlation was found using method 3 index. Focusing on the postoperative samples, no correlation was found between the vWF multimer pattern, nor vWF antigen, and the echocardiographic parameters studied. Additionally, an analysis of the vWF multimer pattern of the 13 patients who had paired pre- and postoperative blood samples, showed no statistical difference on the vWF multimer pattern, nor in the vWF antigen levels.

In conclusion, vWF multimer pattern correlated with several echocardiographic parameters used to evaluate aortic stenosis severity, namely the mean and maximum transaortic gradients. Among the analysis methods used, method 3 revealed to be the most suitable, presenting stronger correlations with both mean and maximal transvalvular pressure gradients.

Keywords: von Willebrand factor, Aortic Stenosis, Transcatheter aortic valve implantation, Surgical aortic valve replacement, Biomarker

RESUMO

A estenose aórtica (EA) é a doença valvular mais frequente e é expectável que a sua incidência suba ao longo dos anos com o envelhecimento da população. A única opção de tratamento passa pela substituição da válvula, que pode ser feita cirurgicamente ou por implantação de prótese percutânea.

Ambas as abordagens têm um risco de regurgitação paravalvular associado, mas este risco é superior na implantação percutânea. A avaliação da severidade da regurgitação paravalvular assim como a da severidade da EA pode ser desafiante apenas por ecocardiografia. Assim, biomarcadores circulantes podem fornecer informações úteis sobre a gravidade da doença e as complicações da AVR.

O fator de von Willebrand (FvW) é uma proteína multimérica que circula no plasma e está envolvida na hemóstase primária e secundária. Os multímeros do FvW circulam no plasma e possuem diversos pesos moleculares; no entanto, com o fluxo turbulento existente na estenose aórtica e na regurgitação paravalvular, os multímeros de elevado peso molecular (MEPM) fragmentam-se o que leva a perda dos mesmos. Os MEPM são os que detêm maior atividade biológica, pelo que a perda destes multímeros compromete o normal processo de coagulação, conduzindo a hemorragias. A perda de MEPM pode ser monitorizada através de uma imunoelctroforese. Após a substituição da válvula aórtica e, na ausência de regurgitação ou com correção da mesma verifica-se uma recuperação do normal perfil multimérico do FvW.

O padrão multimérico do FvW foi avaliado numa coorte de doentes que foram submetidos a substituição da válvula aórtica por via cirúrgica, com objetivo de comparar o padrão multimérico do FvW antes e depois da cirurgia. Foi ainda avaliado o potencial do padrão de vWF como biomarcador da severidade da estenose aórtica. A coorte foi composta por 30 doentes, dos quais se obteve amostras de sangue antes e após cirurgia em 13 casos.

Nesta tese, o padrão multimérico do FvW foi avaliado por três estratégias distintas. O primeiro método utilizou como medida as intensidades máximas do perfil multimérico do FvW. O segundo método consistiu em contar os MEPM. Finalmente, o terceiro método usou o fator de retardação como medida de perda dos MEPM. Adicionalmente, o índice dos MEPM do doente, dividido pelos MEPM de uma amostra controlo foi calculado para todos os métodos. A correlação de todos os indicadores do padrão multimérico de FvW com parâmetros ecocardiográficos, rotineiramente usados para avaliar a severidade da EA, foi avaliada.

Considerando apenas as amostras de pré-operatório (N = 30), este estudo encontrou correlações entre o padrão multimérico de FvW e os parâmetros ecocardiográficos que

avaliam a gravidade da EA, nomeadamente o gradiente transvalvular médio e gradiente máximo. O método 2, assim como o seu índice, não permitiu o estabelecimento de correlações entre o perfil multimérico do FvW com nenhuma das variáveis estudadas. A análise feita com os métodos 1 e 3, assim como o índice do método 1, correlacionaram o perfil multimérico do FvW com o gradiente médio ($r=-0.359$, $p=0.051$; $r=-0.564$, $p=0.001$; $r=-0.409$, $p=0.02$ respetivamente). Adicionalmente, o perfil multimérico do FvW correlacionou-se com o gradiente máximo aquando da análise pelo índice do método 1 e do método 3 ($r=-0.428$, $p=0.03$; $r=-0.572$, $p=0.002$; respetivamente). O índice do método 3 não estabeleceu qualquer tipo de correlação entre o perfil multimérico do FvW e os outros parâmetros ecocardiográficos usados para avaliar a severidade da EA. Considerando apenas as amostras de pós-operatório, não foi encontrada qualquer tipo de correlação entre o padrão multimérica FvW, ou o antigénio e os parâmetros que avaliam a EA. Adicionalmente, a análise aos 13 doentes que possuíam amostras de pré e pós-operatório emparalhadas, não evidenciou diferenças no FvW, seja no seu padrão multimérico seja nos níveis de antigénio.

Em conclusão, o padrão multimérico de FvW correlacionaram-se com parâmetros ecocardiográficos que avaliam a severidade da estenose aórtica, nomeadamente, os gradientes médio e máximo, conseguida através da análise pelo método 3, apontando este método como o mais adequado.

Palavras-Chave: Fator de von Willebrand, Estenose Aórtica, Regurgitação Paravalvular, Implantação Percutânea, Substituição cirúrgica valvular aórtica, Biomarcador

LIST OF FIGURES

Figure 1. Time-course of VWF multimer patterns in two patients observed before, 24 h, one month and six months after surgery. Small multimers are at the bottom, large forms at the top. Note the correction of the VWF abnormalities and the presence of ultra-large VWF multimers not usually found in normal plasma, starting from 24 h postoperative. The normal VWF multimer pattern persisted up to the 6th month. Adapted from³⁸ 11

Figure 2. von Willebrand Factor domains, dimer and multimer structure. A) Basic monomer of vWF with respective domains, binding sites, and functions B) Dimer structure of vWF and C) multimer structure of vWF..... 15

Figure 3. Protocol for the optimization of platelet poor plasma. Created with Biorender.com 23

Figure 4. Platelet density (cells per μL) of the different centrifugations conditions evaluated in the first assay, represented by the letters A, B, C, D, at CP1 (left) and CP2 (right). All groups included plasma from 6 healthy volunteers. Values are represented as Mean \pm SD. Statistical analysis by Friedman test followed by Dunn's multiple comparison test. * $p < 0.05$, and ** $p < 0.005$ 30

Figure 5. Platelet density (cells per μL) of the different centrifugations evaluated in the second assay, represented by the letters W, X, Y, Z, at CP1 (left) and CP2 (right). All groups included plasma from 5 healthy volunteers. Values are represented as Mean \pm SD. Statistical analysis by Friedman test followed by Dunn's multiple comparison test. 32

Figure 6. Agarose gel of vWF normalized by the amount of total protein. Lanes 1 to 8 are samples from healthy volunteers while lanes 9 to 14 are samples from AVS patients. 33

Figure 7. Slot Blot membrane, with total protein stain (left) versus probing with vWF antibody (right). Lanes 1 through 8 correspond to samples of healthy volunteers while 9 through 13 are samples from patients with AVS. 34

Figure 8. Agarose gel of vWF normalized via Slot Blot. Lanes 1 through 7 are samples from healthy volunteers while lanes 8 through 12 are samples from patients with AVS. 35

Figure 9. Agarose gel of vWF normalized via vWF absolute quantification. Lanes 1 to 13 are samples from patients with AVS while lane 14 corresponds to a healthy volunteer, serving as reference. Lanes 2, 3, and 4 are preoperative samples which are paired in with their respective postoperative sample in lanes 7, 6 and 5 respectively. Lanes 1, 8, 9, 10, and 11 refer to unpaired preoperative samples. 36

Figure 10. Agarose gel of vWF comparing a subset of samples quantified by both relative (left), and absolute quantification (right). Samples 1, 2, and 3 are samples from patients with AVS. Sample 4, and 5 correspond to a healthy control. The full gel image is in supplementary figure 3 (relative quantification). For absolute quantification, the full gel image is present in Figure 9 (left), and supplementary figure 4 (right). 37

Figure 11. Correlation of vWF multimer profile with AVS parameters. The vWF HMWM multimer ratio (left), its index (center), and loss of HMWM (%) (right) with the mean transvalvular pressure gradient (mmHg). The lines present in the graphs are regression lines. Each dot represents a patient. Correlation coefficients, and p values are represented at the right top corner of each graph..... 40

Figure 12. Correlation of vWF multimer pattern with AVS parameters. The vWF HMWM multimer ratio index (left), and loss of HMWM (%) (right) with the aortic valve maximum pressure gradient (mmHg). The lines present in the graphs are regression lines. Each dot represents a patient. Correlation coefficients, and p values are represented at the right top corner of each graph. 41

Figure 13. vWF multimer pattern evaluated by the HMWM loss (%) (left) and total vWF antigen (right) in the 13 paired samples before and after aortic valve replacement. 44

SUPPLEMENTARY FIGURES

Supplementary figure 1. Plasma of a healthy volunteer when submitted to different test conditions for PPP obtention. On the left plasma that was submitted to 150 g for 10 minutes (test condition C), and on the right 2100 g for 15 minutes (test condition D). 54

Supplementary figure 2. Slot blot membrane with total protein staining (top) and vWF (bottom). Samples 1 to 15 are from patients with AVS, while samples 15 and 16 are from healthy volunteers. Samples are triplicated vertically. The reference sample is in lane 2..... 55

Supplementary figure 3. Agarose gel of vWF normalized via relative quantification. Samples 1 through 8 are from patients with AVS, and samples 9 through 11? are samples from healthy volunteers. Sample 3, 4 and 5 correspond to sample 1, 2 and 3 in Figure 10, in the results section. Samples 10, and 11 correspond to samples from healthy volunteers 4 and 5 respectively in Figure 10..... 56

Supplementary figure 4. Agarose gel of vWF normalized via absolute quantification. Samples 1 through 14 are samples from patients with AVS. Sample 15 is from a healthy volunteer. Sample 5 was excluded from the analysis due to the inability of extracting the vWF multimer pattern. 57

Supplementary figure 5. Agarose gel of vWF normalized via absolute quantification. In gel A, healthy volunteers are in lanes 1,2 and 3 while in gel B, healthy volunteers are in lanes 11, 12 and 13. Lastly, in gel C only one sample of a healthy volunteer was placed in lane 14. In gel A preoperative samples are in lanes: 9, 10, 11, 12, 13, and are paired with postoperative samples in lanes: 8, 6, 4, 5, 7 respectively. In gel B preoperative samples are in lanes: 1, 2, 3, 4, 5 and are paired with postoperative samples in lanes: 7, 6, 8, 9, 10 respectively. Samples 1 in gel B was reloaded in gel C in lane 1. Lastly in gel C preoperative samples are in lanes: 2, 3, 4 and are paired with postoperative samples in lanes: 7, 6, 5 respectively. Lanes 8 through 11 are from preoperative samples. 58

LIST OF TABLES

Table 1. Classification of aortic valve stenosis severity and the defining echocardiographic measurements, according to the European Society of Cardiology ^{23,24}	5
Table 2. Classification of aortic stenosis severity according to mean transaortic pressure gradient, aortic valve area, left ventricle ejection fraction, and stroke volume ²⁵	6
Table 3. von Willebrand Disease types, mutation responsible for the phenotype and main characteristics. Data from ^{32,35,37}	9
Table 4. von Willebrand Disease and Acquired von Willebrand Syndrome diagnostic tests. Data from ^{31,35,36}	13
Table 5. Variables tested to obtain the platelet poor plasma	22
Table 6. Cell densities (cells per μL) obtained with the four tested conditions, after the first (CP1) and second centrifugation (CP2). Data is presented as mean \pm SD.	29
Table 7. Cell densities (cells per μL) obtained with the four tested conditions. after the first (CP1) and second centrifugation (CP2). Data is presented as mean \pm SD.	31
Table 8. Baseline characteristics of the study population.	38
Table 9. Spearman correlations between the VWF multimeric profile. as assessed by different methods. and different clinical variables associated with the severity of aortic stenosis before aortic valve replacement. Significant correlations are highlighted.	42
Table 10. Postoperative correlations between the VWF multimeric profile as assessed by different methods. and different clinical variables associated with the severity of the disease after valve replacement.	43

SUPPLEMENTARY TABLES

Supplementary table 1. Solutions used for the analysis of vWF multimers. 59

LIST OF ABBREVIATIONS

A

AA	Amino Acid
ACEI	Angiotensin-converting enzyme inhibitors
ADAMTS-13	A disintegrin-like and metalloprotease domain with thrombospondin type-motif, number 13
ADAM28	A disintegrin-like and metalloprotease domain-containing protein 28
ARB	Angiotensin receptor blockers
AAS	Acetylsalicylic acid
AVS	Aortic Valve Stenosis
AvWS	Acquired von Willebrand Syndrome
AVR	Aortic Valve Replacement

B

BAV	Bicuspid Aortic Valve
BNP	B-type natriuretic peptide

C

CAVD	Calcific aortic valve disease
CMR	Cardiac Magnetic Resonance
CP1	Control Point 1
CP2	Control Point 2

E

ER	Endoplasmic Reticulum
----	-----------------------

F

FVIII:C	Factor VIII coagulation assay
---------	-------------------------------

G

GpIb	Platelet receptor glycoprotein Ib
GpIIb/IIIa	Platelet receptor glycoprotein IIb/IIIa

L

LV	Left Ventricle
----	----------------

O

OD Optical Density

OPG Osteoprotegerin

P

PPP Platelet-Poor Plasma

PR Paravalvular Regurgitation

R

RANKL Receptor Activator of Nuclear Factor Kappa-B Ligand

Rf Retardation factor

S

SAVR Surgical Aortic Valve Replacement

T

TAVI Transcatheter Aortic Valve Implantation

TBS Tris Buffer Saline

TBS-T Tris Buffer Saline with Tween

U

UL-MWM Ultra large-Molecular Weight Multimers

V

VECs Valve endothelial cells

VEGF Vascular endothelial growth factor

VICs Valve interstitial cells

vWD von Willebrand Disease

vWF von Willebrand Factor

vWF:Ag von Willebrand Factor Antigen

vWF:CB von Willebrand Factor collagen binding

vWF:MD von Willebrand factor multimer distribution

vWFpp von Willebrand Factor propeptide

vWF:RCo von Willebrand Factor ristocetin assay

W

WPB Weibel Palade bodies

DEFINITIONS

A

Aortic valve area (cm²)

Opening area (orifice) of the aortic valve

Maximum gradient (mmHg)

Maximal difference in pressure between the left ventricle and the aorta in systole

L

Left ventricle ejection fraction (%)

Ratio of left ventricle stroke volume to left ventricle end-diastolic volume

Left ventricle mass index

Left ventricular mass normalized to the body surface area

Left ventricle stroke volume

Volume of blood pumped by the left ventricle during systole

M

Mean transvalvular pressure gradient (mmHg)

The mean difference in pressure between the left ventricle and the aorta in systole

P

Peak velocity

Peak velocity of blood flow through the aortic valve during systole

S

Stroke Volume

Volume of blood pumped out of the LV during systole

V

Velocity Ratio

Ratio between peak velocity in the left ventricle outflow tract and peak velocity through the aortic valve, in systole

PREAMBLE

Valvular heart disease is one of the leading causes of cardiovascular mortality and morbidity. The most common valve disease in the developed world is aortic valve stenosis, resulting from a progressive fibro-calcification of the valve. Treatment options are limited to surgery or intervention to replace the diseased valve by a new prosthetic valve; however, these procedures are not risk-free and can result in paravalvular regurgitation. The management of aortic stenosis is also difficulted by a very prolonged asymptomatic phase, and definitive diagnosis is only possible by cardiac imaging, especially using echocardiography. von Willebrand factor circulates in plasma in multimers of different sizes. Under high shear stress states, like in aortic stenosis, the larger multimers are more susceptible to degradation. The multimeric profile of vWF is thus emerging as a potential biomarker of aortic valve stenosis severity and will be the main focus of this thesis.

Introduction

Calcific Aortic Valve Disease: Epidemiology and Risk Factors

Calcific aortic valve disease (CAVD) is the most prevalent valve disease in the western world, affecting approximately 2% of people over 60 years of age¹. The disease progresses slowly and can remain asymptomatic for decades. Patients may even be asymptomatic with moderate and severe forms of the disease, however after symptoms onset, the 2-year mortality rate is approximately 50%².

CAVD is characterized by remodeling and progressive calcification of the aortic valve². This process was first thought to be passive and a natural consequence of aging³. However, now it is known to be an active degenerative process, starting with valve sclerosis, meaning the thickening of the valve, due to lipid deposition, and progressing towards a fibrotic, and calcified valve. This results in the narrowing of the aortic valve, clinically classified as aortic valve stenosis (AVS), compromising its function and, thus, impairing blood flow^{2,4}.

In the developed world, CAVD is the main cause of AVS, while in developing countries rheumatic heart disease remains the main cause. The latter is the result of an infection by *Streptococcus pyogenes*, which involves an auto-immune response, where auto-antibodies attack, among others, endocardial structures⁵. The exact trigger for the degenerative form of AVS is not known, but some risk factors have been established, such as the male gender, hypercholesterolemia, hypertriglyceridemia, diabetes mellitus, hypertension, and smoking²⁻⁴. Furthermore, congenital bicuspid valves (BAV), a disorder affecting approximately 1%-3% of the population⁶, is also a known risk factor for degenerative AVS.

Pathophysiology of CAVD

A healthy aortic valve is composed of three leaflets (tricuspid), which, in turn, are composed of three different layers: fibrosa, spongiosa, and ventricularis. The outer layer facing the aorta, the fibrosa, is composed mainly of collagen, while the middle layer, the spongiosa, is constituted by glycosaminoglycans and proteoglycans². Lastly, the ventricularis which faces the left ventricle is constituted by collagen and elastin fiber. Their different compositions translate into distinct functions. The fibrosa provides mechanical strength, while the spongiosa absorbs some of the mechanical stress generated by the cardiac cycle⁴ and keeps the outer layer lubricated, and, lastly, the ventricularis provides compliance by distributing radial forces⁴. Two main cell types compose the aortic valve: valvular endothelial cells (VECs) and valvular interstitial cells (VICs). VECs line the outer layers of the valve and are responsible for maintaining valve integrity, acting as a physical barrier between the aortic valve and the blood⁷. These cells are also fundamental to keep tissue homeostasis, being the first sensors of environmental changes, such as changes in shear stress, and releasing several paracrine

factors, such as nitric oxide, an important cell messenger involved in vasodilatation. VECs are also an important source of von Willebrand factor (vWF). In turn, VICs compose a heterogeneous set of cells, which are essential to maintain the integrity of the extracellular matrix (ECM) of the valve². These cells are usually in a quiescent state unless they become activated, as occurs in CAVD. This can happen due to injury or abnormal mechanical stress, the latter especially pronounced in BAV⁸.

The initiation stage of CAVD resembles the pathogenesis of atherosclerosis, with endothelial damage, caused by mechanical stress, being accepted as the initial event. The damage leads to a disruption of the VEC layer, which allows the infiltration of low-density lipoprotein (LDL) that, with time, become oxidized⁴. Both oxidized lipids and endothelium damage lead to the upregulation of adhesion molecules in the endothelium, namely vascular cell adhesion molecule-1 and intercellular adhesion molecule-1². Upregulation of adhesion proteins by the endothelium leads to a greater adhesion of immune cells, specifically monocytes, which in the valve differentiate into macrophages⁵.

Once in the valve, the uptake of oxidized lipids triggers the activation of the innate immune response, which is mediated through toll-like receptors (TLR)/Nuclear Factor Kappa B (NF- κ B) pathways^{4,9}. Several molecules can activate the NF- κ B canonical pathway namely: tumor necrosis factor (TNF), interleukin-1 β (IL-1 β), and reactive oxygen species. This activation leads to the expression and release of pro-inflammatory cytokines like interleukin-6 (IL-6)⁹, which can activate valvular interstitial cells (VICs).

Activated VICs increase the deposition of collagen and the expression of matrix metalloproteinases (MMPs) and shown enhanced proliferative and migratory activity. The result is ECM remodelling and fibrosis. With the perpetuation of the injury/mechanical stress, activated VICs can also differentiate into a myofibroblastic and osteoblastic phenotype¹⁰.

Initially, VICs osteoblastic differentiation is stimulated by macrophages inflammatory cues; however, as the disease progresses, VICs become independent of external stimuli for differentiation². Several molecular pathways contribute to this differentiation. IL-6 mediates this transition through bone morphogenetic protein 2 (BMP-2), receptor activator of NF- κ B ligand (RANKL) and the Notch pathways. In the bone, the RANKL pathway promotes osteoclast differentiation and bone resorption, thus releasing calcium and phosphate into the bloodstream. Osteoprotegerin (OPG) is an antagonist of the RANKL pathway: by binding to RANKL, OPG inhibits binding to RANK and, thus, osteoclastic differentiation. Contrary to what happens in the bone, in the valve this pathway is considered to induce VICs osteoblastic transformation. Moreover, in the valve of patients with AVS, OPG is not present in significant

amounts¹¹. Upregulation of BMP-2 in VICs also contributes to their differentiation¹¹. Altogether BMP, Notch and the RANKL pathway induce an osteoblastic transformation in VICs which results in increased expression of alkaline phosphatase and osteocalcin^{2,11}. This leads to calcium deposition by VICs and subsequent valve calcification. Moreover, apoptosis of valve cells also contributes to calcification by creating nucleation sites for microcalcification⁴. Additionally, VECs can also differentiate into VICs via epithelial to mesenchymal transition, which in turn can acquire an osteoblastic phenotype.

Valve calcification only leads to more inflammation, immune system activation, cell death, and further differentiation of VICs which, again, leads to more calcification. With calcification and fibrosis, the valve becomes stiffer and stiffer, increasing shear stress and obstructing blood flow from the left ventricle⁴. This in turn, has detrimental effects on the myocardium. As the valve narrows, blood flow is hampered, leading to an increase in afterload, an increase in the pressure that the left ventricle must exert to pump blood. To compensate for the added pressure, the left ventricle (LV) hypertrophies. This adaptive response to increased pressure is, in an initial stage, needed to maintain LV function; however, eventually LV hypertrophy leads to dysfunction, caused by myocardial apoptosis and fibrosis, and, ultimately, heart failure. In fact, LV mass has been correlated with an increased mortality risk⁸.

Management and Treatment of CAVD

Why is surgery/intervention the only option?

Due to the nature of AVS pathophysiology, initially driven by lipid deposition in a way similar to atherosclerosis, and the fact that risk factors for the development of the disease include high levels of cholesterol, lipid-lowering therapy aiming at stalling the progression of AVS was subjected to clinical trials¹². This was supported by previous retrospective studies, where the use of statins (a class of lipid-lowering therapies) was associated with a halted progression of AVS¹³⁻¹⁵. However, in clinical trials the results were conflicting. Only the Rosuvastatin Affecting Aortic Valve Endothelium (RAAVE) trial showed an improvement in echocardiographic AVS parameters, but it was a rather small study comprising only 121 patients¹⁶. Other clinical trials, such as the Scottish Aortic Stenosis and Lipid-Lowering Trial, Impact on Regression (SALTIRE) and the Simvastatin and Ezetimibe in Aortic Stenosis (SEAS), showed that statins did not halt or decrease AVS progression^{12,17}. One reason might be that in these patients, the disease was simply too advanced for there to be any benefit from statin therapy, since lipid deposition is a driver event in AVS. Nevertheless, even when statin therapy was initiated in patients with asymptomatic mild or moderate AVS, the results were equally disappointing, as shown by the Aortic Stenosis Progression Observation: Measuring

Effects of Rosuvastatin (ASTRONOMER) trial¹⁸. Additionally, in the retrospective studies and RAAVE trial, only patients with AVS and hypercholesterolemia were treated, while in other clinical trials, such as SALTIRE, SEAS, and ASTRONOMER these patients were excluded, which may explain the discrepant results^{18,19}.

After statins failure, denosumab and bisphosphonate alendronic acid were subjected to clinical trials²⁰. Denosumab is a monoclonal antibody that inhibits the RANKL pathway, which, as previously mentioned, promotes the osteoblastic differentiation of VICs. In turn, bisphosphonate alendronic acid inhibits osteoclastic activity and is used in the treatment of osteoporosis^{11,20,21}. Unfortunately, both failed in halting AVS progression. So, even after multiple clinical trials, there are currently no pharmacological treatments available to stop or slow the progression of AVS²² with treatment relying solely on valve replacement.

Diagnosis and classification of AVS

Aortic valve stenosis is a silent disease that can remain asymptomatic for years. Patients are often diagnosed when symptoms such as angina, dizziness, and syncope develop or when auscultation reveals a systolic murmur. Additionally, the diagnosis can also be an incidental finding when patients are referred to an echocardiogram for other purposes²³. Thus, specific biomarkers that can detect the disease are lacking. The diagnosis, classification, and monitorization of AVS is performed exclusively using imaging techniques, with a single blood biomarker to aid in the timing of surgical intervention.

Table 1. Classification of aortic valve stenosis severity and the defining echocardiographic measurements, according to the European Society of Cardiology^{24,25}.

Aortic stenosis severity	Mean transaortic pressure gradient (mmHg)	Peak Velocity (m/s)	Aortic valve area (cm²)	Velocity ratio
<i>Aortic Sclerosis</i>	-	≤ 2.5	-	-
<i>Mild</i>	< 30	2.6 – 2.9	1.5	0.50
<i>Moderate</i>	30 - 40	3.0 – 4.0	1.0 – 1.5	0.25-0.50
<i>Severe</i>	> 40	> 4.0	< 1.0	<0.25

Echocardiogram is the gold standard for diagnosing and assessing AVS, which is classified according to its severity in mild, moderate, or severe. For this, three main echocardiographic parameters are considered namely, aortic valve area, mean transaortic pressure gradient, and lastly, the peak velocity (Table 1)²⁴. Other parameters such as velocity ratio, stroke volume

and parameters that evaluate LV function such as, LV mass, and LV ejection fraction (%) are also used^{24,25}. In addition to this, stroke volume, and LV ejection fraction are used to further subdivide AVS into two main categories, high gradient, and low gradient (Table 2)²⁶.

In addition to echocardiogram, other imaging techniques such as computed tomography to assess calcium score,²⁷ and cardiac magnetic resonance (CMR), which can accurately quantify LV fibrosis, provide additional information that can aid in the diagnosis and prognosis of the patient. Calcium score predicts disease progression and clinical events²⁸, and LV fibrosis is associated with an adverse prognosis. Additionally, in asymptomatic patients, stress imaging can help unmask the symptoms and more accurately determine AVS severity²⁵.

Table 2. Classification of aortic stenosis severity according to mean transaortic pressure gradient, aortic valve area, left ventricle ejection fraction, and stroke volume²⁵.

	Subtype	MG (mmHg)	PV (m/s)	AVA (cm ²)	LVEF	SV
High-Gradient AVS	<i>Classical Low-Flow</i>	≥ 40	≥ 4.0	<1	< 50%	
	<i>Paradoxical Low-Flow</i>				≥ 50%	< 35 ml/m ²
	<i>Normal-Flow</i>					≥ 35 ml/m ²
Low-Gradient AVS	<i>Classical AVS</i>	< 40	-	≤ 1	< 50%	
	<i>Paradoxical Low-Flow</i>				≥ 50%	< 35 ml/m ²
	<i>Normal-Flow</i>					≥ 35 ml/m ²

Abbreviations; AVA, Aortic valve area; AVS, Aortic valve stenosis; MG, Mean pressure gradient; LVEF, left ventricle ejection fraction; SV, Stroke volume

Currently the only blood-based biomarker established in AVS is the B-type natriuretic peptide (BNP)²⁵. BNP is a hormone secreted by cardiomyocytes in response to increased ventricular volume. Abnormal levels of this blood biomarker, and its N-terminal pro-form (NT-proBNP), can predict symptom-free survival and are associated with clinical adverse outcomes²⁹.

Generally, for patients with severe AVS, valve replacement is advised whether the patient is symptomatic or not. In asymptomatic patients with severe AVS and LV dysfunction, early intervention is recommended²⁵. However, for asymptomatic patients without indicators of an

adverse prognosis, there is still an ongoing debate whether it is better to intervene earlier rather than later when the patient becomes symptomatic^{25,28}.

TAVI versus SAVR

Aortic valve replacement can be done through open-heart surgery, normally referred to as surgical aortic valve replacement (SAVR) or, transcatheter aortic valve implantation (TAVI). Both carry associated risks and are indicated for different patient populations.

The more invasive approach, SAVR, is usually performed in younger patients (<65 years) with few or no surgery-associated risk factors and few comorbidities, while TAVI is performed in older patients (>75 years)²⁵, with comorbidities and / or surgery-associated risk factors. TAVI itself consists of the implantation of a bioprosthetic valve, without the removal of the native valve. The most common approach is femoral TAVI, in which the catheter is inserted into the femoral artery. Once in place, the prosthetic valve is released, expands, creates a seal, and takes over the native valve function²⁸. This approach carries less mortality risk for patients, but the risk of paravalvular regurgitation (PR) is greater, due to a potential lack of seal between the valve and the patient anatomy²⁸. PR is one of the major drawbacks of TAVI, and patients with considerable leaks are more symptomatic, and have a lower life expectancy^{30,31}. Patients with moderate to severe leaks require re-intervention. Pacemaker implantation is also higher in patients submitted to TAVI when compared to SAVR²⁵.

In the case of SAVR the native valve is removed, and a mechanical valve is put in place via open heart surgery. Although the risk of PR is lower than with TAVI, mechanical valves require a long-term anticoagulation regimen. Severe bleeding risk, acute kidney injury and atrial fibrillation are more common in patients submitted to SAVR²⁵ when compared with TAVI patients. In addition, SAVR is much more invasive than TAVI and requires a longer convalescence period. Both procedures carry the risk of thromboembolism and endocarditis²⁸.

von Willebrand Disease: History, epidemiology, and disease subtypes

vWD was first described in 1926 by Eric von Willebrand, a Finnish physician, while studying an inherited bleeding disorder in consanguineous families from Föglö, located in the Åland islands^{32,33}. The first reported case was from a 5-year-old girl, Hjördis S. who has had several episodes of severe bleeding following tooth extraction and trivial wounds. Four of her sisters had died of severe bleeding between the ages of two and four³⁴. Still, it was only in 1961 that vWD was found to be caused by the lack of a plasma factor and in 1970 that vWF

was isolated from plasma. One year later, it was found that patients with vWD lacked this factor in their plasma³⁴.

vWD affects 0.1 to 1% of the population, making it the most common bleeding disorder. Most types of the disease exhibit an autosomal dominance pattern, however, due to incomplete penetrance, some vWD patients may remain asymptomatic³⁵ (Table 2). In clinical terms, patients may present with nose bleeds, gastrointestinal bleeding, heavy menstrual periods along with bleeding after dental procedures, childbirth, and surgeries^{35,36}. Severe bleeding, for instance in the gastrointestinal tract from angiodysplasia, dilated, and abnormal blood vessels, is most common in elderly patients with type 2 or 3 vWD^{32,35}. These two types of vWD also present with moderate to severe mucocutaneous bleeding that can be life threatening³⁵.

Type 1 vWD is the most common subtype accounting for 70%³⁷ of vWD cases and is characterized by a low quantity of vWF in plasma. Type 1 can still be further subdivided into type 1C that encompasses patients whose cause of vWF deficiency is increased clearance³⁵. Type 2 accounts for 25% of cases and is associated with a more severe bleeding phenotype³⁵. This type is further subdivided in 2A, B, N, and M and is characterized by qualitative defects in vWF, higher susceptibility to cleavage by ADAMTS-13, or enhanced binding to platelet receptors, among others. Lastly, type 3 is the rarest and most severe subtype that accounts for less than 5% of cases of vWD. Like type 2 vWD, this type is characterized by severe mucocutaneous bleeding^{32,35}. Type 3 is marked by an almost complete deficiency in vWF. In-depth characteristics of each subtype as well as inheritance patterns and mutations that give rise to the disease are summarized in Table 2.

Treatment of vWD

The treatment of vWD is essentially pharmacological and the drugs used can be subdivided into three main categories: Antifibrinolytics, desmopressin and FVIII/vWF concentrates. Treatment choice depends on vWD type and bleeding severity. Antifibrinolytics such as tranexamic acid and ϵ -aminocaproic acid can be useful for minor bleeding episodes or for preventing bleeding episodes. These agents inhibit fibrinolysis and can be used in combination with other therapies. Desmopressin acts by stimulating the release of vWF, increasing the factor levels in the plasma. This treatment is best indicated for type 1 vWD, but patients must first be subjected to a desmopressin trial to guarantee an adequate response³⁵. FVIII/vWF concentrates are indicated for severe bleeding in all vWD types, and can also be used when desmopressin is contraindicated³⁵.

Table 3. von Willebrand Disease types, mutation responsible for the phenotype and main characteristics. Data from ^{32,35,37}

Type	Inheritance Pattern	Genetic mutation/domain affected	Outcome	General Type Characteristics
1	Autosomal dominant	Null alleles	Decreased plasma concentration of vWF due to reduced synthesis of normal vWF	Partial quantitative deficiency of normal vWF
		Various mutations along the protein coding gene	Rapid clearance (Type 1C) or intracellular retention of vWF	
2A	Autosomal dominant	Missense mutations in propeptide D3, and A2 domains Several A1 domain mutations have also been described	Impaired multimerization Loss of HMWM	Qualitative defects in vWF
		Missense mutations in CK domain	Impaired dimerization	
		Missense mutations in A2 domains	Increased susceptibility to cleavage by ADAMTS13	

2B	Autosomal dominant	Missense mutations in the A1 domain (gain-of-function) Few mutations have been reported in the D3 domain	Increased affinity to Gplb α binding site, spontaneous binding to Gplb α and loss of HMWM	
2M	Autosomal dominant	Missense mutations in the A1 domain	Reduced affinity of vWF for Gplb α and reduced collagen binding	
		Missense mutations in the A3 domain	Reduced collagen binding	
2N	Autosomal recessive	Missense mutations in the D'D3 domain	Reduced affinity of vWF for factor VIII Defective multimerization	
3	Autosomal recessive	Null alleles	Undetectable or very low levels of vWF in plasma	Almost complete quantitative deficiency of vWF

Abbreviations: ADAMTS13, A disintegrin-like and metalloprotease domain with thrombospondin type-motif, number 13; HMWM, High molecular weight multimers; Gplb α , Platelet receptor glycoprotein Ib α ; vWF, von Willebrand Factor;

Acquired von Willebrand Syndrome

Unlike vWD, which is the most common inherited blood disorder affecting up to 1% of the population, acquired von Willebrand syndrome (AvWS) is a rare bleeding disorder with unknown incidence³⁸. This syndrome arises from structural or functional alterations of the vWF that are not inherited. These include autoantibodies against vWF, reduced synthesis of vWF (mimicking type 1 vWD), adsorption on the surface of cells or platelets, and increased shear stress, which in turn, causes increased vWF (mimicking type 2A vWD). The diversity of the phenotypes is explained by different underlying causal factors. For example, hypothyroidism leads to a reduced synthesis of vWF, while in systemic lupus erythematosus, autoantibodies against vWF are generated. Lymphoproliferative disorders are the most common cause of AvWS, and in this case, vWF is adsorbed into circulating cells^{35,38}.

Furthermore, cardiovascular disease is thought to account already for 40 to 45% of all cases of AvWS. In conditions like AVS or congenital heart defects, the characteristic high shear stress states increase the susceptibility of vWF to proteolysis, leading to a reduction in its plasmatic levels (Figure 1). The higher prevalence of cardiovascular disease associated AvWS is probably explained by to the growing implantation of left ventricular assisted devices, and by higher reporting rates from cardiologists, who are becoming more aware of this condition^{38,39}.

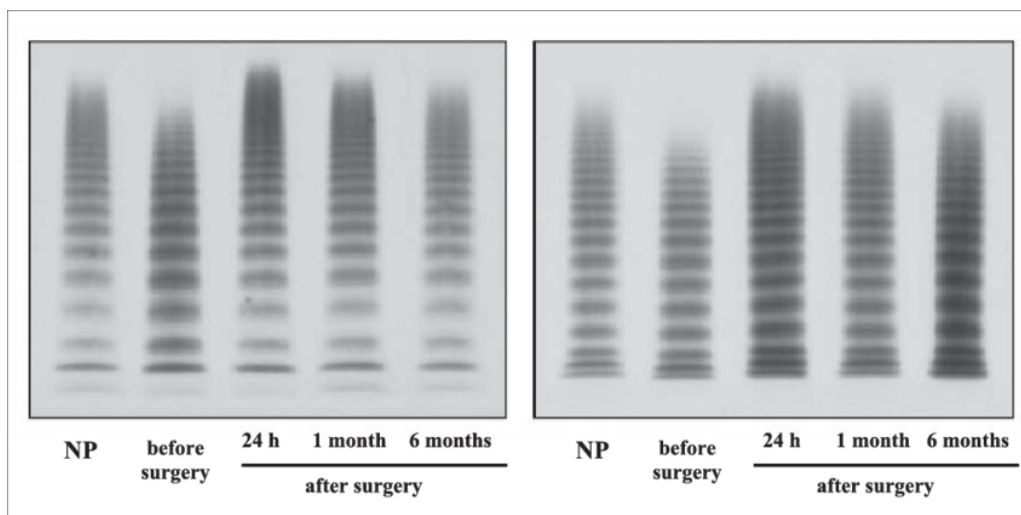


Figure 1. Time-course of VWF multimer patterns in two patients observed before, 24 h, one month and six months after surgery. Small multimers are at the bottom, large forms at the top. Note the correction of the VWF abnormalities and the presence of ultra-large VWF multimers not usually found in normal plasma, starting from 24 h postoperative. The normal VWF multimer pattern persisted up to the 6th month. NP, Normal pattern. Adapted from⁴⁰

Other situations can lead to the development of AvWS such as extracorporeal oxygenation. In all these cases, AvWS is caused by high shear stress that leads to the loss of the vWF multimers (Figure 1). Regardless of the mechanism, all these diseases increase the risk of bleeding, and treatment relies on treating the underlying cause of AvWS³⁹.

Diagnostic tests for vWD and AvWS

Several laboratory tests exist to evaluate vWF and aid in the diagnostic of both vWD and AvWS. Patient history of bleeding as well as a family history of bleeding are important factors to take into consideration in the differential diagnosis of vWD. In the case of AvWS, new-onset bleeding is the most important factor to account for, as AvWS is secondary to an existing condition^{36,38}.

To test for vWD an initial panel of recommended screening tests include vWF:Ag, a platelet-dependent vWF activity test, and Factor VIII coagulant activity³⁶ (Table 4). With the confirmation of vWD, other tests must be done to identify the vWD subtype. These include vWF multimer distribution (vWF:MD), low-dose RIPA, vWF-FVIII binding assay, vWF collagen binding assay (vWF:Co), vWF propeptide/vWF antigen (vWFpp/vWF:Ag). Lastly, a desmopressin challenge test, and even genotyping, may be useful in distinguishing specific subtypes of vWD.

In the case of AvWS, vWF:Ag, vWF:RCo, and vWF: CB cannot rule out the diagnosis of AvWS, since the results of these tests can be within reference levels. In this way, patients may not present with a reduction in antigen levels or in the vWF activity, and still have AvWS³⁹. For this reason, a multimer analysis is recommended. The distribution of multimers seen in AvWS patients with AvWS is present in Figure 1^{38,40}. The tests used, and their function is explained in Table 4.

Table 4. von Willebrand Disease and Acquired von Willebrand Syndrome diagnostic tests. Data from^{31,35,36}

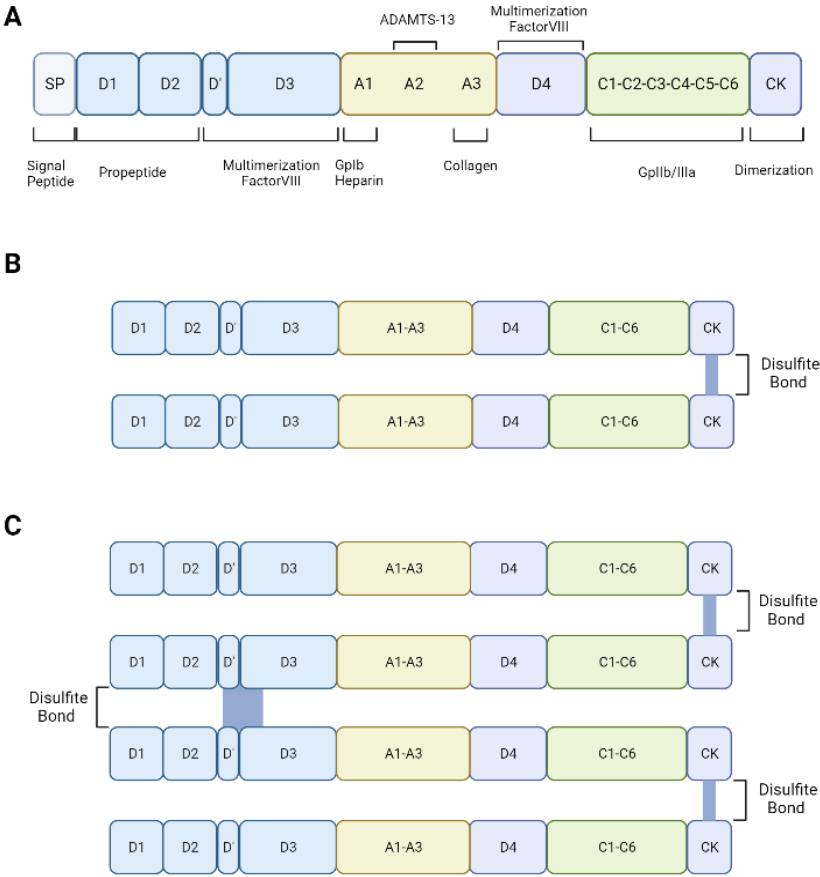
Laboratory Test	Function
<i>vWF:Ag</i>	Quantifies vWF total levels in the plasma
<i>vWF:RCo</i> or <i>vWF:GPIbR</i>	Measures the ability of vWF to bind to GPIb and agglutinate platelets in the presence of the antibiotic ristocetin. Ristocetin is thought to force vWF conformation to change, much like in high shear stress conditions, facilitating vWF binding to platelets, in the absence of shear stress <i>vWF:GPIbR</i> is a similar test which uses wild-type GPIb-coated latex beads instead. This test is also performed in the presence of ristocetin
<i>Low dose RIPA</i>	Similar to <i>vWF:RCo</i> , but with lower concentrations of ristocetin. In normal patients vWF will not aggregate in the presence of ristocetin at low concentration. Useful for confirmation of type 2B disease, where vWF aggregates platelets even at low ristocetin concentrations, due to an increase affinity for GPIb
<i>VWF:GPIbM</i>	Variation of the <i>vWF:RCo</i> , <i>vWF:GPIbR</i> and low dose RIPA tests, using a recombinant GPIbM carrying gain-of-function mutations that allow binding to vWF without ristocetin. Thus, <i>VWF:GPIbM</i> also assesses the binding of vWF to platelet receptors.
<i>vWF:CB</i>	Measures vWF ability to bind to collagen
<i>vWF:RCo/vWF:Ag</i>	Ratio of vWF platelet-binding activity to antigen in the plasma
<i>vWF:CB/vWF:Ag</i>	Ratio of vWF collagen-binding activity to antigen in the plasma
<i>FVIII:C</i>	Quantifies FVIII total levels in the plasma
<i>vWF:FVIII</i>	Assesses the ability of vWF to bind to exogenous FVIII

<i>vWFpp/vWF:Ag</i>	Assesses the level of vWF maturation, by assaying the ratio of propeptide levels to antigen levels (mature vWF) in the blood
<i>vWF:MD</i>	Assesses the multimer pattern of vWF present in the plasma by agarose gel electrophoresis. For this, patient plasma is centrifuged to obtain platelet poor plasma (PPP). A sample of PPP is subjected to an electrophoretic run, which separates vWF multimers by their molecular weight. Multimer distribution can then be analyzed on a membrane or by in gel immunofixation and quantified using densitometry analysis. This is a demanding technique with high variability between laboratories. Still, it is indispensable in the diagnosis of both vWD and AvWS
<i>Desmopressin challenge</i>	Usually done after a vWD diagnosis to assess an adequate response to the treatment, however, this test may also be done to diagnose Type 1C vWD. First, baseline vWF parameters, such as vWF antigen and FVII total values are assessed. Next desmopressin is administered, followed by the assessment of the previous parameters at 1, 2 and 4 hours. A response is considered adequate if vWF levels rise 2 to 4-fold

Abbreviations; FVIII, factor VIII; GPIb, glycoprotein Ib; PPP, Platelet poor plasma; vWD, von Willebrand Disease; vWF, von Willebrand Factor; vWF:Ag, von Willebrand Factor Antigen; vWF:CB, von Willebrand Factor collagen binding assay; vWF:FVIII von Willebrand factor binding to FVIII; vWF:MD, von Willebrand factor multimer distribution; vWFpp, von Willebrand Factor propeptide; vWF:RCo, von Willebrand Factor ristocetin assay.

von Willebrand Factor: The molecular basics

von Willebrand factor is a large multimeric glycoprotein present in plasma. The vWF gene is encoded in the short arm of the chromosome 12p13.2 and it is synthesized as a pre-pro-peptide of 2813 amino acids (aa)³³. Following synthesis, vWF pre-pro-peptide is translocated into the endoplasmic reticulum (ER), where the signal peptide is cleaved off^{41,42}. Additionally, pro-vWF undergoes glycosylation and dimerization in the ER. vWF suffers extensive glycosylation, with the mature peptide containing 12 N-linked glycosylation sites and 10 O-linked glycosylation sites, and the propeptide containing an additional 3N-linked glycosylation sites^{33,43,44}.



Created in BioRender.com bio

Figure 2. von Willebrand Factor domains, dimer and multimer structure. A) Basic monomer of vWF with respective domains, binding sites, and functions B) Dimer structure of vWF and C) multimer structure of vWF.

More than 90% of these glycans are capped by sialic structures. Additionally, ABO(H) blood group determinants are also present in both N- and O-linked glycans^{43,44}. These determinants play a role in the clearance of the factor, which is discussed further ahead. Following correct dimerization and glycosylation, the maturation of the factor encompasses multimerization in the Golgi complex⁴¹⁻⁴³. The propeptide is cleaved by furin in the trans-Golgi network, but remains non-covalently linked to mature vWF, being important for vWF multimerization. The propeptide is believed to catalyze disulfide bond formation between the D3 domains⁴³, although the propeptide disulfide isomerase activity has not been directly demonstrated^{33,43}. Notwithstanding, the deletion of the propeptide prevents vWF multimerization^{33,37}. The mature protein consists of 2050 aa and 250kDa and is constituted by multiple domains in the following order: D1-D2-D'-D3-A1-A2-A3-D4-C1-C2-C3-C4-C5-C6-CK (Figure 2)^{35,43,45}. Domains D1 and D2 compose the propeptide, while D'-D3-A1-A2-A3-D4-C1-C2-C3-C4-C5-C6-CK constitute the mature peptide. CK domains are fundamental for vWF dimerization. Similarly, D'-D3 are important for vWF multimerization as well as for binding and stabilizing factor VIII^{35,43,45}. Two monomers combine to form a dimer, and two dimers form a multimer through disulfide bonds between the CK and D'-D3 domains, respectively⁴⁶. Additionally, multimers can also combine, giving rise to very large structures, some with up to 10.000 kDa^{42,46}. vWF multimers can interact with many proteins involved in hemostasis. For instance, A1 domain binds to platelet receptor glycoprotein Ib (GpIb). Similarly, the C1 domain binds to the platelet receptor glycoprotein IIb/IIIa (GpIIb/IIIa). Additionally, the A1 domain binds to collagen and heparin^{35,47}. The heparin-binding site was also shown to bind to vascular and platelet growth factors in animal studies⁴⁸. Lastly, the A3 domain binds to exposed collagen (Figure 2).

It is important to mention that genetic mutations in these domains give rise to von Willebrand Disease (vWD) and affect several aspects of the protein biology, such as dimerization, multimerization, and even vWF clearance^{33,35}. More than 750 unique mutations have been reported³⁷. Of note, vWF A2 domain holds a specific cleavage site (1605Tyr-1606Met) for ADAMTS-13 (disintegrin-like and metalloprotease domain with thrombospondin type-1 motif, number 13). When exposed to this protease, vWF very large multimers can be fragmented to smaller multimers, resulting in a varying loss of biological activity, with immediate hemostatic implications^{35,43}.

von Willebrand Factor: an important regulator of hemostasis

vWF is synthesized in megakaryocytes and endothelial cells, including VECs. It is stored in Weibel-Palade bodies (WPB) in endothelial cells or in α -granules, in the case of

platelets^{41,43}. The formation of WPB is completely dependent on vWF synthesis. vWF is stored in a ratio of 1:1 propeptide : mature vWF and is also released into the plasma in this ratio³³.

Not only the vWF storage but also its release differs between cell types. Endothelial cells release the factor constitutively. It is estimated that around 95% of the factor is released this way. Platelets, on the other hand, only release the factor when activated^{42,49}. Furthermore, endothelial cells release vWF in response to various stimuli such as fibrin, thrombin, histamine, inflammatory response, adrenergic stress, and vascular damage^{33,50}. Desmopressin, a pharmacological agent used in the treatment of vWD, also stimulates the release of vWF^{41,42}.

vWF exists as a multimeric protein of various sizes: ultra-large (>10000 kDa), high (5500-10000 kDa), intermediate (3000-5000 kDa), and low molecular weight (500-2500 kDa) isoforms²². This factor is stored in ultra-large molecular weights (UL-MWM), while low, intermediate, and high molecular weight multimers are constitutively secreted into the plasma by endothelial cells^{42,49}. The UL-MWM are only released upon endothelial activation or vascular injury⁵¹.

Upon its release to the plasma, in physiological conditions, vWF remains in a globular or quiescent form⁴². However, upon vascular injury, and due to the high fluid shear stress, the vWF unfolds and assumes a stretched conformation⁴⁷. This change in conformation exposes the vWF domains, favoring collagen binding to the A3 domain. Then, vWF mediates platelet adhesion to the endothelium⁴⁷ (through Gplb α binding to A1) and aggregation (through GpIIb/IIIa binding to C1). This forms the initial platelet plug. vWF is also responsible for carrying Factor VIII to the site of vascular injury as well as for stabilizing it, increasing its half-life, and consequently promoting coagulation^{35,47}. The high molecular weight multimers (HMWM) of vWF are the most biological active and therefore the best at mediating these interactions^{42,52}. Therefore, it is evident the essential role of vWF in hemostasis.

Once in circulation, vWF multimers are exposed to the action of metalloproteinases, which are key players in the regulation of multimer size, and, indirectly, their biological activity. ADAMTS-13 is a metalloproteinase, which is synthesized mainly in hepatic stellate cells, and its best-known biological function is the regulation of vWF multimer size, and consequently, its activity. Under physiological conditions, vWF remains in its globular conformation, and is resistant to ADAMTS-13 proteolysis. However, when stretched, vWF is susceptible to cleavage by ADAMTS-13^{42,47}. By cleaving vWF into smaller multimers, ADAMTS-13 decreases vWF hemostatic activity as mentioned above. It should be noted that, like vWF, ADAMTS-13 is not only involved in hemostasis, but also plays a significant role in inflammation and angiogenesis⁵³.

UL-MWM are not usually found in circulation since ADAMTS-13 rapidly cleaves UL-MWM into smaller multimers. This is because the UL-MWM are hyperactive and mediate spontaneous platelet adhesion, which can result in platelet agglutination^{42,54}. Not surprisingly, an inherited or acquired deficiency, due to autoantibodies against ADAMTS-13 leads to thrombocytopenia purpura in which platelet-rich microthrombi can block arterioles and capillaries⁵³⁻⁵⁶. Not all UL-MWM are released into the plasma. Some molecules are constitutively released to the basal membrane and remain tethered to the endothelial surface forming string-like structures^{56,57}. Much like the globular vWF, endothelium-bound UL-MWM also unfold and expose their domains, under high shear stress conditions^{56,57}, being susceptible to ADAMTS-13 cleavage, and originating smaller HMWM^{53,57}. These isoforms have the greater affinity for platelet receptors^{47,52}.

Besides ADAMTS-13, vWF is also cleaved by Thrombospondin-1 (TSP-1) and by ADAM28, a member of the ADAM (A Disintegrin and Metalloproteinase) family. Thrombospondins are a family of glycoproteins involved in angiogenesis and cell-to-cell communication. TSP-1 controls vWF multimer size by cleaving the disulfide bonds that link the factor subunits and may compete with ADAMTS-13 *in vivo*, blocking its action⁵¹. The ADAM family is composed of large membrane-anchored proteases that are involved in intracellular communication, adhesion, and that, more recently, have been found to play a role in cancer and its progression⁵⁸. ADAM28 was found to cleave vWF, protecting cancer cells from vWF-induced apoptosis, thus promoting cancer cell survival⁵⁸.

Mature vWF has a long and variable half-life in the plasma circulating for 8 to 12 hours. This variability may be explained by the presence of blood-type determinants since A and B antigens may protect against clearance of the factor. Indeed, O blood types have 25% lower levels of vWF^{43,59}. Age is another determinant of the amount of vWF circulating in plasma. As age increases, vWF also increases. Clearance of vWF occurs through endocytosis by macrophages and by hepatocytes⁴⁴.

Less Known roles of vWF

In addition to its well-known role in hemostasis, vWF also plays an important role in immunity, inflammation, and angiogenesis. UL-MWM strings facilitate the attachment and rolling of leukocytes to the endothelium, and, thus, their extravasation, aiding in the inflammatory response^{53,56}. Additionally, neutrophils and other leukocyte populations can also bind to vWF⁶⁰. vWF is an acute-phase protein, and in response to inflammatory stimuli, it is released from endothelial cells' WPB. This leads to an increase of vWF levels with inflammation and, not surprisingly, in several inflammatory diseases⁵⁰.

The factor also plays a role in cancer. As previously mentioned, cleavage by ADAM28 protects cancer cells from vWF-mediated apoptosis; however, other studies have linked higher vWF plasma levels to metastases and cancer progression as well as a poorer prognosis. This was observed across a variety of cancer types⁶¹, and may be mediated by the binding of cancer cells to vWF and platelets, using them as a vehicle for metastasis. Indeed, specific tumor cells have been shown to express vWF *de novo*⁶⁰.

Lastly, vWF also plays a role in angiogenesis, as a negative regulator. Two mechanisms have been proposed. When bound to $\alpha\beta 3$ integrin, a receptor involved in angiogenesis, vWF inhibits Vascular Endothelial Growth Factor Receptor-2 (VEGFR-2), and consequently VEGFR-2 induced proliferation of endothelial cells. Also, the absence of vWF leads to defective formation of WPB and results in improper storage of Angiopoietin-2 (Ang2). This leads to Ang-2 binding to the Tie2 receptor, a tyrosine kinase receptor, promoting vessel permeabilization and destabilization⁶². Unsurprisingly, angiodyplasia, has been described in patients with vWD^{62,63}, particularly in the nose, nail bed, prostate and in the gastrointestinal tract⁶².

von Willebrand factor in Aortic Valve Stenosis

Focusing on AVS, the increase in vWF proteolysis is a result of the high shear stress caused by the stenotic aortic valve. As previously mentioned, high shear stress unfolds vWF, making this protein more prone to ADAMTS-13 proteolysis, resulting in the loss of HMWM (AvWS)³⁹. HMWM loss is thought to affect 40% to 50% of AVS patients⁶⁴⁻⁶⁶. This impairs hemostasis, leading to bleeding episodes, such as in the gastrointestinal tract. The coexistence of gastrointestinal bleeding, AvWS, and AVS is a clinical entity termed Heyde syndrome. It is important to note that upon a successful valve replacement, HMWM are recovered, and consequently, the bleeding episodes disappear in the majority of the patients with Heyde syndrome⁶⁶. These observations reinforce the need for further research on the diagnostic and prognostic potential of vWF.

Several prospective studies have been conducted. Van Belle *et al.*⁶⁷ analyzed the vWF multimer pattern in 183 AVS patients before and after TAVI to test if aortic regurgitation during TAVI can be monitored through the analysis of vWF multimer profile. They found that the vWF multimer ratio only normalized after TAVI, for patients without aortic regurgitation. Moreover, they found that vWF HMWM recovered in patients whose aortic regurgitation was later successfully corrected, but not in patients with persistent regurgitation. Importantly, this index correlated with higher mortality at 1 year⁶⁷. Moreover, besides vWF multimer ratio, other vWF indexes, for instance, vWF antigen/activity ratios, are also associated with mortality and

periprocedural bleeding risk. In the Indexes of von Willebrand Factor as Biomarkers of Aortic Stenosis Severity study⁶⁸, patients (N=60) with a lower vWF activity/antigen ratio (<0.8) and with loss of HMWM showed an increased risk of aortic valve replacement or mortality. Additionally, vWF multimer ratio and vWF activity/antigen ratio also correlated with the severity of AVS, measured by echocardiographic parameters such as mean transvalvular gradient⁶⁸. An additional study with a cohort of 50 patients also demonstrated that vWF abnormalities increased with the mean transvalvular pressure gradient⁶⁹. On the contrary, Sedaghat, A. *et al.* found no correlation between the vWF activity, antigen, and antigen/activity ratio with aortic stenosis severity in a cohort of 74 patients undergoing TAVI. However, a correlation between periprocedural bleeding, bleeding that occurs during or within 48 hours of the intervention, and a lower vWF activity/antigen ratio was found⁶⁴. Patients with a lower vWF activity/antigen ratio had an increased risk of periprocedural bleeding. The discrepancies in the correlation of vWF and AVS severity, could be due to different ways to analyze the vWF multimer pattern, and due to different inclusion criteria for patients, since some studies only include patients with severe AVS⁷⁰. Still, so far, vWF has shown promise as a useful biomarker in the evaluation, prognosis of AVS as well as in the detection of paravalvular regurgitation.

Aims

There is still an unmet need for a reliable biomarker in AVS which can accurately help physicians to appraise AVS severity. In this sense, vWF multimer analysis has been proposed as a useful biomarker; however, the studies conducted so far are contradictory. Some studies report that the loss of the HMWM in the vWF multimer pattern is correlated with severity of the disease^{64,68}, while one study did not find such correlation⁷⁰.

Thus, the general aim of this work is to assess the correlation of the vWF multimer pattern with echocardiographic indexes of AVS severity in a cohort of patients submitted to AVR. More specific aims include to:

- ✓ Optimize plasma sample preparation and vWF multimer analysis.
- ✓ Assess the relationship of vWF profile with echocardiographic indexes of AVS severity.
- ✓ Establish a ratio/measure of vWF multimers that would allow to effectively assess AVS severity.
- ✓ Determine the prognostic relevance of vWF multimer profile in postprocedural paravalvular regurgitation and periprocedural bleeding risk.
- ✓ Better characterize von Willebrand acquired syndrome.

Materials and methods

Sample collection and ethics statement

Aortic stenosis patients undergoing AVR, or on occasion of a postoperative consultation were invited to participate in this study. A blood sample was collected just before surgery or during the programmed follow-up consultation. This study followed the principles stated in the Declaration of Helsinki, and the ethics committee of the Centro Hospitalar Universitário de São João (CHUSJ) approved the protocol (reference CEC109-2020). Informed consent was obtained from all patients. Control samples were obtained by donation from healthy volunteers. In total, 30 preoperative plasma samples were used, of these, 13 were paired with their respective postoperative plasma samples.

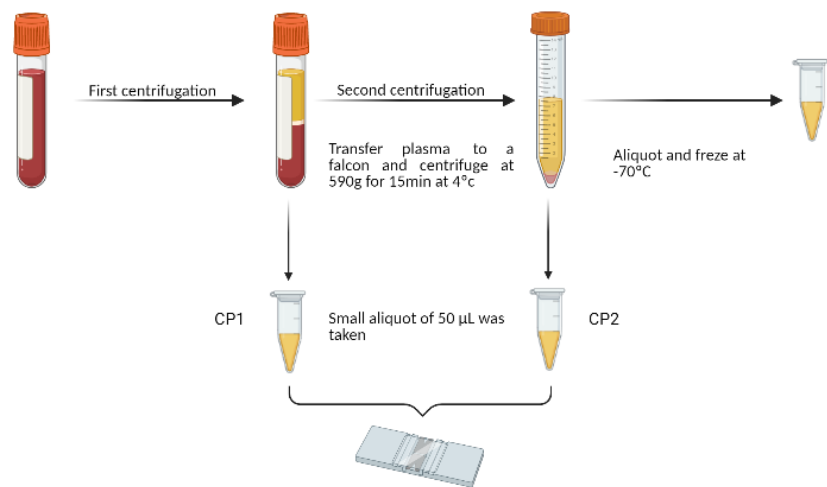
Platelet-poor plasma protocol optimization

To obtain platelet-poor plasma several conditions were tested. All conditions tested are represented in table 5 and an experimental design is represented in Figure 3. First, the impact of the first centrifugation on the number of platelets/cellular debris was assessed, fixing the conditions of the second centrifugation (590 g, 10 min), except for the reference condition A. In any case, the temperature was fixed at 18°C. After testing the first four conditions (First Assay in table 5), the one that yielded the lower number of cells densities was further optimized.

Table 5. Variables tested to obtain the platelet poor plasma

First Assay			
<i>Condition</i>	<i>First centrifugation (g/min)</i>	<i>Second centrifugation (g/min)</i>	<i>Temperature</i>
A	400/10	800/10	18°C
B	380/15	590/10	
C	150/10		
D	2100/15		
Second Assay			
<i>Condition</i>	<i>First centrifugation (g/min)</i>	<i>Second centrifugation (g/min)</i>	<i>Temperature</i>
W	2100/15	590/5	18°C
X		590/30	
Y		590/15	
Z		590/15	4°C

In a second assay, both the temperature and the duration of the second centrifugation were changed to obtain the lowest number of cells (second assay in table 5). In any case, blood was drawn from healthy volunteers to tubes and processed immediately. Four plasma tubes with a capacity of 4 mL were drawn from each volunteer and allowed to cool to room temperature. Next, the plasma tubes were equilibrated in a water bath to 18°C for 30 minutes and then submitted to the first centrifugation. Afterwards, a small aliquot was taken for counting (Control Point 1 (CP1)), and the remaining plasma was then carefully transferred to a falcon tube and submitted to a second centrifugation step. A small aliquot was again taken for counting (Control Point 2 (CP2)).



Created in BioRender.com 

Figure 3. Protocol for the optimization of platelet poor plasma. Created with Biorender.com

The remaining plasma was aliquoted and frozen at -70°C, discarding the last 1/3 of the plasma. The exact same procedure was done when testing for temperature and duration of the second centrifugation. Platelets were manually counted using a Neubauer chamber.

vWF relative quantification through Slot Blot analysis

The analysis of the vWF multimer profile through gel immuno-electrophoresis requires normalization of the plasma volume to the amount of total vWF antigen. In a first attempt, relative quantification of vWF was performed by slot blot analysis. First, total plasma protein was measured using a bicinchoninic acid protein assay kit (Pierce™ BCA Protein Assay Kit, Thermo Scientific™, Catalog number 23225). For this, plasma samples were diluted 1:100. Then, the volume of plasma equivalent to 5 µg of protein was diluted in tris buffer saline (TBS)

and loaded onto a slot blot apparatus. A vacuum pump was used to transfer the samples onto a nitrocellulose membrane (0.45 µm), pre-activated with 10% methanol. After transfer, the membrane was rinsed with water. To control for the differences in protein transfer, a normalization protocol was followed using Revert™ 700 Total Protein stain (P/N: 926-11010) according to the manufacturer's protocol. Signal detection was performed in an Odyssey apparatus (LI-COR® Biosciences) using the 700 nm channel. Next, total protein stain was removed using Revert Destaining Solution, blocked in 1% BSA for 30 minutes or, alternatively, overnight, followed by incubation with the primary anti-human vWF antibody (Dako, USA A0082) (1:10000). The membrane was then washed three times in tris buffered saline with 0.05% tween (TBS-T) for 10 minutes and incubated with the respective secondary antibody goat anti-Rabbit IgG (LI-COR®, Biosciences, catalog number 926-32211) (1:10000). Lastly, the membranes were washed again with TBS-T and scanned using the Odyssey apparatus in the 800 nm channel. Densitometry analysis was done using Image Studio Lite Version 5.2 (LI-COR®, Biosciences).

Next, the electrophoretic profile of various samples was evaluated by loading the same amount of protein (266 µg) for several plasma samples into a gel. The sample with the best resolution of its multimeric pattern, a good band separation and definition, was chosen as a reference sample. Using this sample as reference, the vWF of the other samples was quantified. For each sample, the vWF signal was normalized to the intensity of total protein (optical density of the previous R700 stain), as:

$$\text{Normalized signal (NS)} = \frac{\text{vWF OD}}{\text{Total Protein OD}}$$

Then, to compare the relative amount of vWF to the reference sample, the normalized vWF signal was divided by that of the reference sample:

$$\text{Ratio} = \frac{\text{NS of the reference sample}}{\text{NS of test sample}}$$

This ratio was then used to correct the protein amount for each sample to obtain the same amount of vWF. Ultimately, different volumes of plasma were processed from each sample to control for vWF being resolved in the gel.

vWF absolute quantification through ELISA

In a second attempt to normalize the amount of vWF for multimer profile analysis, the absolute levels of this protein in PPP were quantified by ELISA (Abcam; catalog no. ab108918), following the manufacturer's instructions.

Assessment of the vWF multimer profile by Immuno-Electrophoresis

The multimer profile of vWF was assessed by immune electrophoresis, based on previously published protocols^{71,72} with modifications. A 2% high gelling (Thermo Scientific™) agarose gel was used instead of a standard polyacrylamide, provided the very high molecular weight of vWF multimers. All the necessary solutions for gel casting and for the electrophoretic run were prepared as already described⁷¹, and are detailed in the appendix (supplementary table 1). A separating and a stacking vertical agarose gel were prepared using a PROTEAN® II xi Cell system (Bio-Rad Laboratories) with several adaptations. Briefly, the system was mounted according to the manufacturer's instructions and checked for leaks with water. Then, an agarose plug was added outside of the system to make the system watertight. To prevent the agarose gel from sliding off the glass plates during the run, a 5% polyacrylamide gel with a height of 1 cm was cast below the separating gel. After polymerization of the polyacrylamide gel, the system and a glass pipette tip were heated to 50°C for 15 minutes. Immediately after heating the system, a 2% (w/V) agarose mixture was poured in between the glass plates using the pre-heated pipette tip. This mixture was allowed to solidify at room temperature. Next, a stacking gel of 0.8% agarose was poured and the wells' comb embedded 0.7 cm down into the gel. The stacking gel was allowed to solidify and the whole system (without removing the comb) was refrigerated at 4°C for, at least, 30 minutes to facilitate comb removal. Next, the wells were washed with electrolyte buffer, the system mounted in the tank, and then checked again for leaks.

Before electrophoresis, plasma samples were diluted in sample buffer (supplementary table 1) according to their vWF:Ag content to a final concentration of 10 U/dL. Then, 10 µL of each plasma samples were incubated for 15 minutes at 60°C. Immediately after, the samples were loaded into the gel. The same reference sample from a healthy volunteer was loaded into all gels. Protein electrophoresis was conducted overnight at 4°C, at 10 mA, for about 15.5 hours. Subsequently, the proteins were fixed on the gel by incubating in a fixing solution (supplementary Table 1) for 1 hour, washed for 30 minutes with distilled water and then another hour with deionized water. Finally, the gel was incubated with the primary antibody (Dako, USA A0082) diluted in antibody buffer (supplementary table 1) (1:10000 – 1:25000) for 4 hours. The gel was then actively washed for 1 hour with TBS-T and kept still overnight in fresh TBS-T. In the following day, the gel was incubated with secondary antibody (LI-COR®, Biosciences, catalog number 926-32211) diluted in antibody buffer (supplementary table 1) (1:10000 – 1:25000) for 4 hours, and then washed in TBS-T for another 3 hours. Finally, the gel was scanned at 800 nm using the Odyssey apparatus. Gel images were reconstituted in

gray scale and analyzed with Image Lab (version 6, Bio-Rad), after converting the scan files to TIFF format.

Analysis of the vWF multimer pattern

Multimers were counted from the bottom of the gel upwards, and the high molecular weight multimers were defined from the 11th band⁴² on, according to the reference sample (healthy volunteer). Since the run is slightly different from gel to gel, and to accommodate for the fact that the number of detected multimers on the reference sample changes, the percentage of HMWM was calculated according to the mode of the number of multimers detected in the reference across all gels, and the threshold band corrected in each gel.

Next, different methods were used to compare the percentage of HMWM across samples:

$$(1) \text{ HMWM} = \frac{\text{Peak Intensity of HMWM}}{\text{Sum of peak intensities of all multimers}}$$

$$(2) \text{ HMWM} = \frac{\text{Number of HMWM}}{\text{Number of all multimers}}$$

$$(3) \text{ HMWM loss (\%)} = Rf (\text{first HMWM}) = \frac{\text{distance run by the first HMWM band}}{\text{gel length}} \times 100 ,$$

with Rf being the Retardation factor or electrophoretic mobility of the first HMWM band. This method was previously described by Hennessy-Strahs, S *et al.*⁷³. Additionally, for all the methods the

$$\text{Index} = \frac{\text{HMWM of the patient}}{\text{HMWM of the healthy control}}$$

was also calculated. This index was previously described by Tamura, T *et al.*⁷⁴.

Statistical Analysis

Continuous data is presented as mean ± standard deviation (SD) and categorical data is presented as absolute frequency (percentage). Normal distribution was tested using the Shapiro-Wilk test. The number of platelets were compared via nonparametric ANOVA (Friedman test) followed by a Dunn's multiple comparison test. A Spearman correlation was performed to measure the correlation between the vWF multimer indexes and the echocardiographic parameters. For the analysis of the paired pre and postoperative samples, a parametric t-test was used, when not normally distributed, a Wilcoxon t-test was used. To evaluate the effect of different types of medication on the vWF measures, an unpaired t-test was used when normally distributed. When not normally distributed a Mann-Whitney test was used. In any case, a $p < 0.05$ was considered significant. All the graphs, and statistical analyses

were performed using GraphPad Prism software version 8.0 (GraphPad Software, San Diego, CA, USA).

Results

Optimization of the protocol to obtain platelet-poor plasma

Since no standard method exists to obtain platelet-poor plasma (PPP), several centrifugations and temperatures were tested to obtain the minimal number of platelets/cellular debris. This is a necessary step to avoid plasma contamination of platelet derived vWF. PPP is, by definition, plasma that has a platelet count of less than 10,000 platelets per μL . Generally, a two-step centrifugation method is used to obtain PPP, where whole blood is centrifuged once (first centrifugation) to obtain plasma, and then, the plasma is subjected to a second centrifugation to obtain PPP.

A brief literature search was conducted, and the conditions annotated only taking into consideration articles that obtained PPP by centrifugating blood twice. From there several conditions were selected taking into consideration different variables such as: centrifugation time, speed, and temperature. For example, articles presenting centrifugations in different units, first centrifugation expressed in g and second in rpm, were excluded. In the end, four main conditions were selected (Table 5).

Primarily, the influence of the first centrifugation in platelets numbers was tested, fixing the second centrifugation at 590 g for 10 minutes, except in condition A (400 g for 10 minutes). This test condition served as a reference, since it had been previously evaluated in a preliminary assay (data not shown).

There were no significant differences when comparing the four different test conditions among themselves at the same time point (Figure 4). However, it is worth to mention that test condition D yielded the lowest mean cell density when compared to the other conditions (Table 6). Additionally, when compared to condition C, a slightly higher volume of plasma, and clearer plasma was obtained with test condition D (Supplementary figure 13 in the appendix).

Table 6. Cell densities (cells per μL) obtained with the four tested conditions, after the first (CP1) and second centrifugation (CP2). Data is presented as mean \pm SD.

	First Assay			
	400 g for 10 minutes (A)	380 g for 15 minutes (B)	150 g for 10 minutes (C)	2100 g for 15 minutes (D)
CP1	127.1 \pm 130.5	122.9 \pm 51.7	258.8 \pm 144.9	58 \pm 67.8
CP2	31.3 \pm 33.3	17.1 \pm 8.6	12.1 \pm 4.9	12.1 \pm 3.9

In a pairwise comparison between the first and second centrifugations, there was a significant reduction in platelet density in conditions B ($p < 0.05$) and C ($p < 0.005$). Again, even though there were no other statistical differences, the mean cell densities were consistently lower at CP2 under all test conditions, suggesting that a second centrifugation is useful in reducing cell numbers. Since the platelet densities were lower in condition D, where the first centrifugation was set at 2100 g for 15 minutes at 18°C, this condition was chosen for further optimization in a second assay. In a second assay (Figure 5), the effect of the duration of the second centrifugation (5 to 30 minutes) and of the temperature (18° vs 4°C) was tested. Like in the first assay, no statistical differences were observed in platelet density after the first and second centrifugations. The same is true when comparing the paired test conditions at the CP1 and CP2 timepoints. Additionally, similarly to the first assay, a second centrifugation consistently resulted in lower mean cell densities (Table 7), but this time, without statistical significance. Interestingly, increasing the centrifugation time did not result in a lower platelet density.

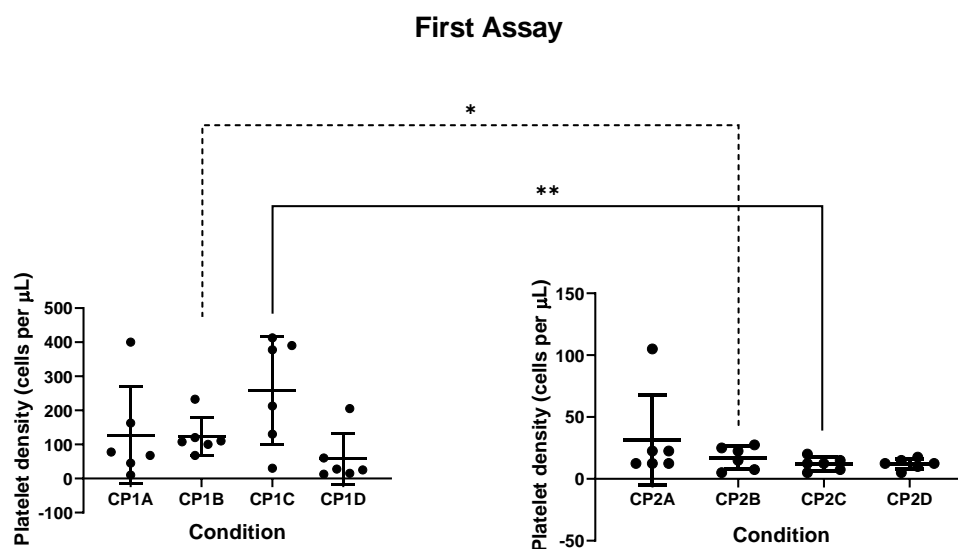


Figure 4. Platelet density (cells per μL) of the different centrifugations conditions evaluated in the first assay, represented by the letters A, B, C, D, at CP1 (left) and CP2 (right). All groups included plasma from 6 healthy volunteers. Values are represented as Mean \pm SD. Statistical analysis by Friedman test followed by Dunn's multiple comparison test. * $p < 0.05$, and ** $p < 0.005$.

Table 7. Cell densities (cells per μL) obtained with the four tested conditions. after the first (CP1) and second centrifugation (CP2). Data is presented as mean \pm SD.

Second Assay				
	<i>590 g for 5 minutes (W)</i>	<i>590 g for 30 minutes (X)</i>	<i>590 g for 15 minutes (Y)</i>	<i>590 g for 15 minutes (Z)</i>
<i>CP1</i>	32 \pm 13.2	46 \pm 33.7	28 \pm 14.8	27 \pm 23.2
<i>CP2</i>	15 \pm 11.3	23 \pm 16.1	15 \pm 6.1	4.5 \pm 4.8

Unlike the duration of centrifugation time which did not impact on cell densities the temperature of centrifugation did. Test condition Z (590 g for 15 minutes at 4°C) produced a lower mean and less variable cell density when compared to the other test conditions. Unlike the first conditions tested, this time no macroscopic difference was seen in terms of plasma quantity or opacity between the test conditions.

It is noteworthy that even after just one centrifugation all test conditions evaluated produced by definition PPP, because the density of cells never surpassed 10000 cells per μL . Furthermore, after the second centrifugation, no matter the condition tested a small pellet of erythrocytes and platelets could sometimes be observed reinforcing the relevance of this step for a downstream vWF analysis.

Second Assay

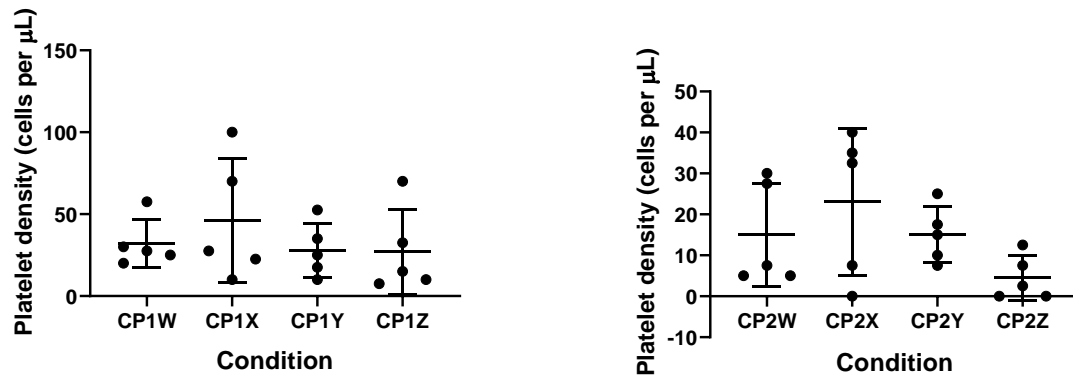


Figure 5. Platelet density (cells per μL) of the different centrifugations evaluated in the second assay, represented by the letters W, X, Y, Z, at CP1 (left) and CP2 (right). All groups included plasma from 5 healthy volunteers. Values are represented as Mean \pm SD. Statistical analysis by Friedman test followed by Dunn's multiple comparison test.

vWF relative quantification through Slot Blot analysis

To relatively quantify vWF several attempts were made since in there is not a universal way of quantifying vWF like one does when quantifying total protein, for example, via BCA before a standard western blot procedure. Indeed, the first attempt at normalizing the vWF quantity in the gel was done via BCA. In this way, all the samples loaded in the gel (Figure 6) had the same amount of total protein (266 µg). In this gel it is visible that even though the same amount of protein was loaded this does not correlate with the amount of vWF detected (green signal). This is especially visible when comparing lanes 1, 2, 3, and 5 which are barely visible with lane 9, in which the same amount of protein led to band overlapping. Still, with this gel allowed us to select sample 12 as a reference sample since it showed a good multimer profile, in other words a good multimer separation, and definition.

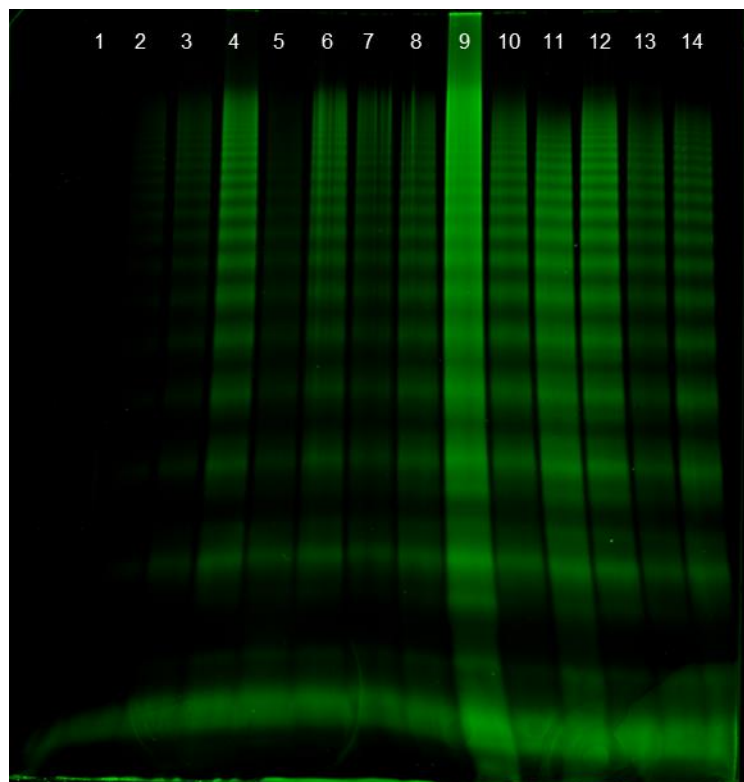


Figure 6. Agarose gel of vWF normalized by the amount of total protein. Lanes 1 to 8 are samples from healthy volunteers while lanes 9 to 14 are samples from AVS patients.

Since total protein assessed by BCA failed as a normalization parameter total vWF was relatively quantified via slot blot. The previous plasma samples were loaded in a slot blot apparatus followed by total protein staining and vWF detection via probing of the membrane with the same antibody (Dako, USA A0082) (Figure 7).

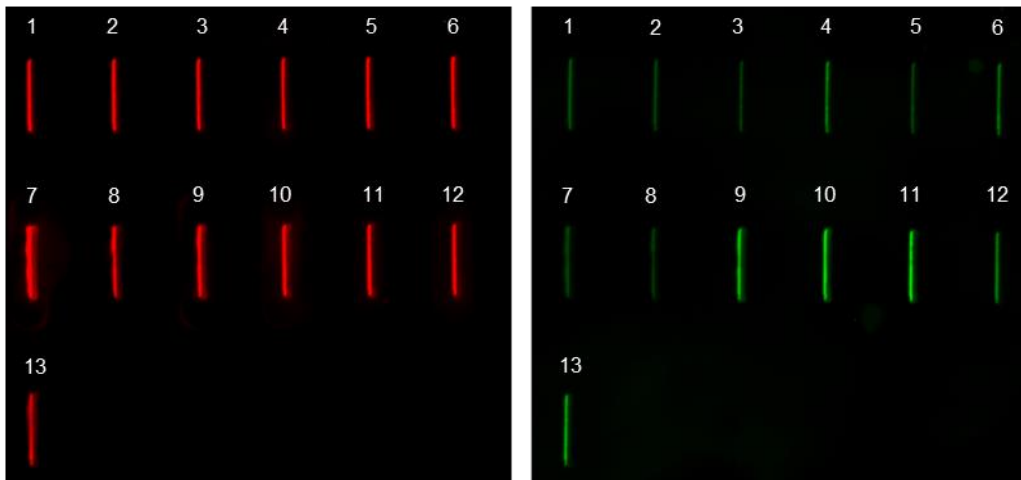


Figure 7. Slot Blot membrane, with total protein stain (left) versus probing with vWF antibody (right). Lanes 1 through 8 correspond to samples of healthy volunteers while 9 through 13 are samples from patients with AVS.

With total protein staining, as expected, no significant differences in the optical density (OD) of the samples were found, however, the same does not happen with vWF signal. Overall, patients had a stronger signal when compared to healthy controls.

A gel was then prepared taken into consideration the relative normalization of vWF. In this gel (Figure 8) several samples were tested mostly without success. Like in the previous gel, some samples were barely visible, lane 2, while in others, such as 4 to 7 the amount of vWF is excessive leading to no bands visible and a strong signal from top to bottom of the gel. Other attempts were made, for example to triplicate all the samples loaded into the slot blot and working with the average of optical densities of the reference sample instead of working with one single replicate. Additionally, alternative reference samples were used, without success.

Despite repeated attempts with different normalization methods neither the normalization via total protein levels nor via vWF relative amount resulted in a satisfactory multimer profile across all lanes. In all cases, total vWF signal was too uneven to conduct multimer profile analysis. Usually, this discrepancy occurred in plasma samples where total protein quantities and vWF signal were at extremes in samples where total protein was the highest, but the vWF signal was low, and vice-versa.

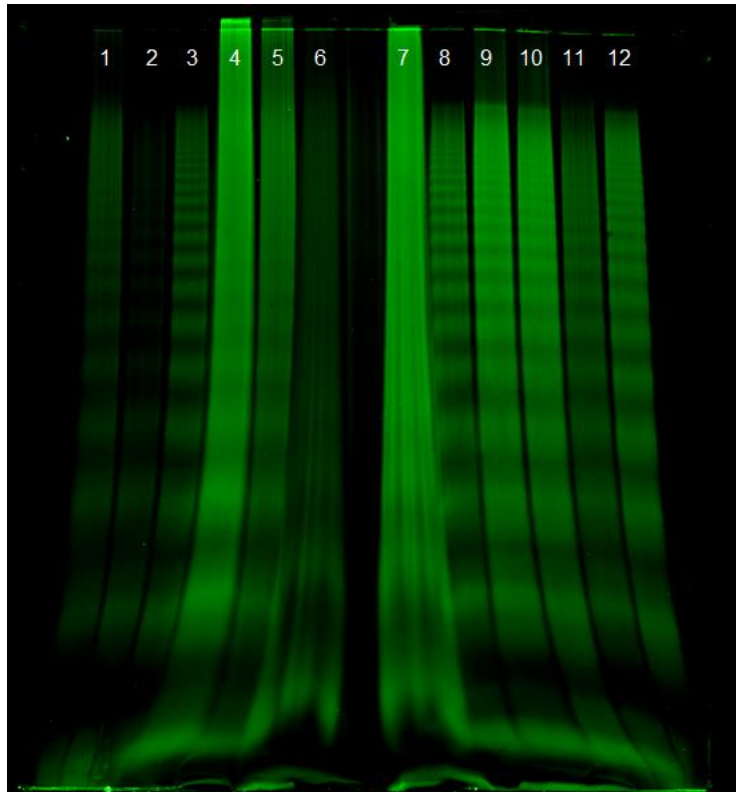


Figure 8. Agarose gel of vWF normalized via Slot Blot. Lanes 1 through 7 are samples from healthy volunteers while lanes 8 through 12 are samples from patients with AVS.

vWF multimer profile analysis after normalization via absolute quantification

Given that it was not possible to use relative quantification to normalize and then analyze the vWF multimer pattern, a different normalization strategy was attempted, this time based on absolute quantification, and using an ELISA. Plasma samples obtained from AVS patients pre- and postoperative were quantified along with samples from healthy volunteers. In any case 10 μ L of plasma samples diluted to 10 U/dL were loaded in the agarose gels. As can be appreciated in Figure 9 the densitometric profile was found to be more homogeneous through this method than by a relative quantification approach.

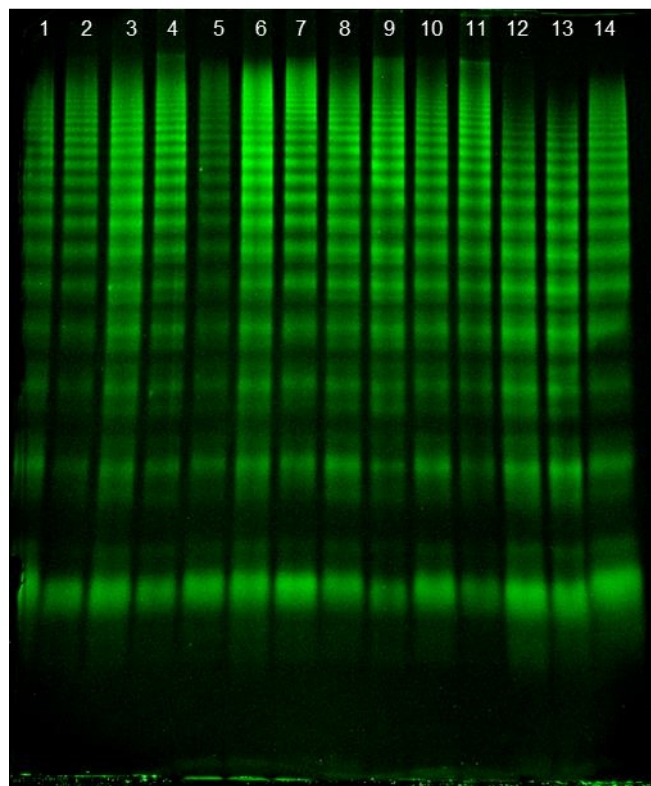


Figure 9. Agarose gel of vWF normalized via vWF absolute quantification. Lanes 1 to 13 are samples from patients with AVS while lane 14 corresponds to a healthy volunteer, serving as reference. Lanes 2, 3, and 4 are preoperative samples which are paired in with their respective postoperative sample in lanes 7, 6 and 5 respectively. Lanes 1, 8, 9, 10, and 11 refer to unpaired preoperative samples.

Even though there were still slight differences in total OD of some samples these did not compromise the analysis of the number of multimers nor its OD. In this gel, sample 5 is clearly fainter than the other samples. Still these samples are still analyzable, since it is possible to extract an adequate multimer profile. Additionally, none of the samples has shown

appreciable band overlap in such a manner that would make the analysis unfeasible. More interestingly is that samples that had previously been semi-quantified and showed no loss of the HMWM appear to have this loss when quantified in an absolute manner. This is true for sample 1 (Figure 10). Other samples, which by the reasons stated above, were not possible to relatively quantify were now easily analyzed (Figure 10).

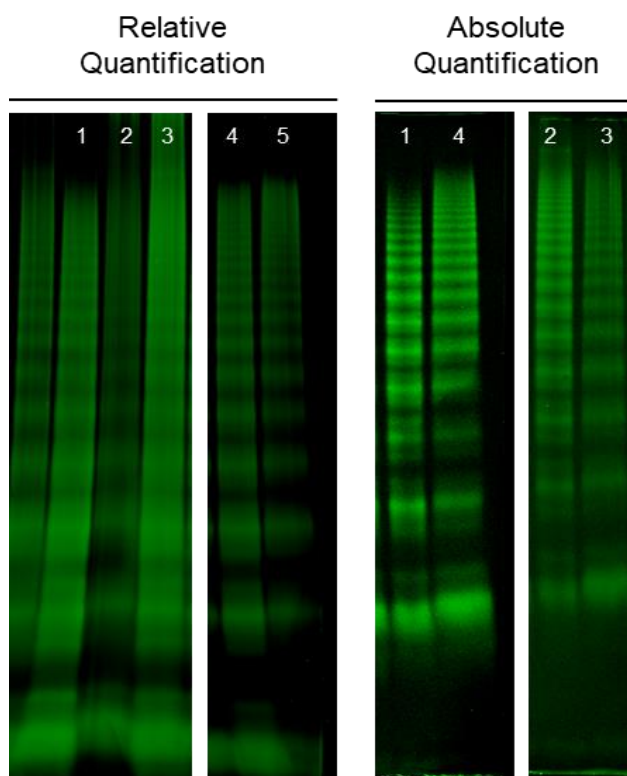


Figure 10. Agarose gel of vWF comparing a subset of samples quantified by both relative (left), and absolute quantification (right). Samples 1, 2, and 3 are samples from patients with AVS. Sample 4, and 5 correspond to a healthy control. The full gel image is in supplementary figure 3 (relative quantification). For absolute quantification, the full gel image is present in Figure 9 (left), and supplementary figure 4 (right).

Can vWF the multimer profile be a biomarker for AVS?

Baseline population characteristics

In total, 30 preoperative plasma samples were used of these 13 were paired with their respective postoperative plasma samples. Preoperative samples were collected the day of the surgery and postoperative samples were collected at the follow-up visit, on average 4 months after the AVR. One sample was excluded from the analyses due to the inability of extracting the multimer pattern (supplementary figure 5). All patients had severe aortic stenosis according to the latest European Society of Cardiology guidelines²⁵, and only one patient had atrial fibrillation. Detailed patient characteristics are present in table 8. It is important to note that in our study 30% of patients had BAV, and that no patient had evidence of postoperative paravalvular leak. Additionally, upon visual inspection of the gels only 5 (16%) samples presented HMWM loss.

Table 8. Baseline characteristics of the study population.

Baseline characteristics	Pre-operative	Post-operative
Age (mean ± SD)	70 ± 7.64	
Male Sex (N / %)	14 (47%)	
BMI. kg/m ² (mean ± SD)	29.26 ± 4.25	
Comorbidities		
CAD (n ^o / %)	11 (36%)	
Diabetes (n ^o / %)	6 (20%)	
Dyslipidemia (n ^o / %)	21 (70%)	
Obesity (n ^o / %)	10 (33%)	
Hypertension (n ^o / %)	26 (87%)	
Lifestyle		
Non-Smoker (n ^o / %)	26 (87%)	
Ex-Smoker (n ^o / %)	3 (10%)	
Smoker (n ^o / %)	1 (3%)	
Medication		

Diuretics (n° / %)	13 (43%)	
Acetylsalicylic Acid (n° / %)	11 (36%)	
Angiotensin-converting enzyme inhibitors (n° / %)	8 (27%)	
Angiotensin receptor II blockers (n° / %)	16 (53%)	
<i>Echocardiographic Findings</i>	Pre-operative	Post-operative
BAV (n° / %)	9 (30%)	-
AV area cm ² (mean ± SD)	0.8 ± 0.14	2.0 ± 0.54
Transvalvular mean transvalvular gradient, mmHg (mean ± SD)	46.7 ± 9.83	12.8 ± 4.59
LVEF. % (mean ± SD)	61 ± 7.33	64.0 ± 5.94

Correlation of the vWF multimeric profile with parameters of disease severity before and after aortic valve replacement

All of the vWF evaluation methods used were correlated with several clinical parameters in a total of 7 echocardiographic parameters. All the variables tested along with the correlation coefficients, and p -values are represented in table 9, and 10. The HMWM intensity ratio (Method 1) and HMWM number ratio (Method 2) evaluated the vWF multimer profile by quantifying the HMWM in each sample indicating that the lower the HMWM in the sample the lower the ratios. Hence, negative correlations are expected with the parameters of AVS severity. Method 3 evaluated the loss of the HMWM via the Rf in a proportional mode, in which the higher Rf, the higher the loss of HMWM. When it comes to correlations with AVS parameters the strongest correlation was found between HMWM loss (%) by method 3, and the aortic maximum gradient ($r=0.572$, $p=0.002$) (Figure 11). This suggests that the higher the loss of HMWM the higher the mean transvalvular gradient.

The HMWM intensity ratio (Method 1) was the one with the lowest correlation coefficients and borderline statistical p values for the association with the AVS parameters. Method 1 index showed a better correlation with both the mean transvalvular pressure gradient ($r=-0.409$; $p=0.02$), and aortic maximum gradient ($r=-0.428$; $p=0.03$) than method 1, indicating the index of patient HMWM divided by the control HMWM correlated better with the pressure gradients than the ratio HMWM alone. In fact, method 1 only correlated with the mean transvalvular pressure gradient ($r=-0.359$; $p=0.051$).

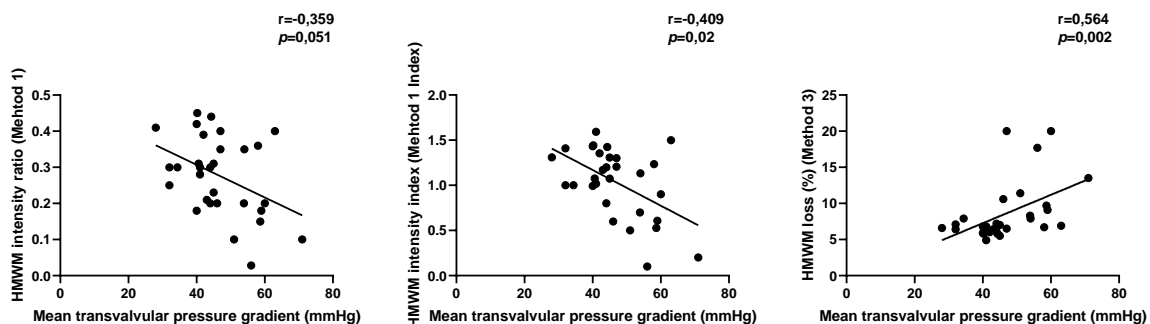


Figure 11. Correlation of vWF multimer profile with AVS parameters. The vWF HMWM multimer ratio (left), its index (center), and loss of HMWM (%) (right) with the mean transvalvular pressure gradient (mmHg). The lines present in the graphs are regression lines. Each dot represents a patient. Correlation coefficients, and p values are represented at the right top corner of each graph.

The HMWM number ratio by method 2, and the respective index did not correlate with any of the AVS severity parameters. Additionally, HMWM loss (%) by method 3 was the one with the strongest correlations overall, additional to its previously mentioned correlation with the maximum gradient HMWM loss (%) also correlated with the mean gradient ($r=0.564$; $p=0.001$) (Figure 12). Remarkably, method 3 index showed no correlations with any of the evaluated parameters.

It is important to mention that all correlations were exclusive for preoperative parameters of disease severity. No correlations were found when between the vWF HMWM profile assessed by various methods with postoperative clinical variables (table 9).

In the study cohort patients take different classes of medications such as diuretics, antiplatelet agents, namely acetylsalicylic acid (AAS), angiotensin-converting enzyme inhibitors (ACEI, and lastly angiotensin receptor II blockers (ARAI). Some medications have been described to alter vWF multimer pattern. Therefore, to rule out any interference of these medications in the vWF profile the latter was compared between patients taking or not taking these drugs. There was no statistically significant difference in the vWF multimer pattern between patients who took these medications when compared to patients who did not take them. Additionally, there was no significant difference in the vWF antigen (U/dL) when comparing patients who took medication compared to patients who did not. This was true for all the medications studied, and for all the different ways of evaluating the vWF multimer pattern, HMWM Loss (%) (Method 3) or HMWM intensities/number ratio (Method 1 and 2 respectively) along with their respective indexes.

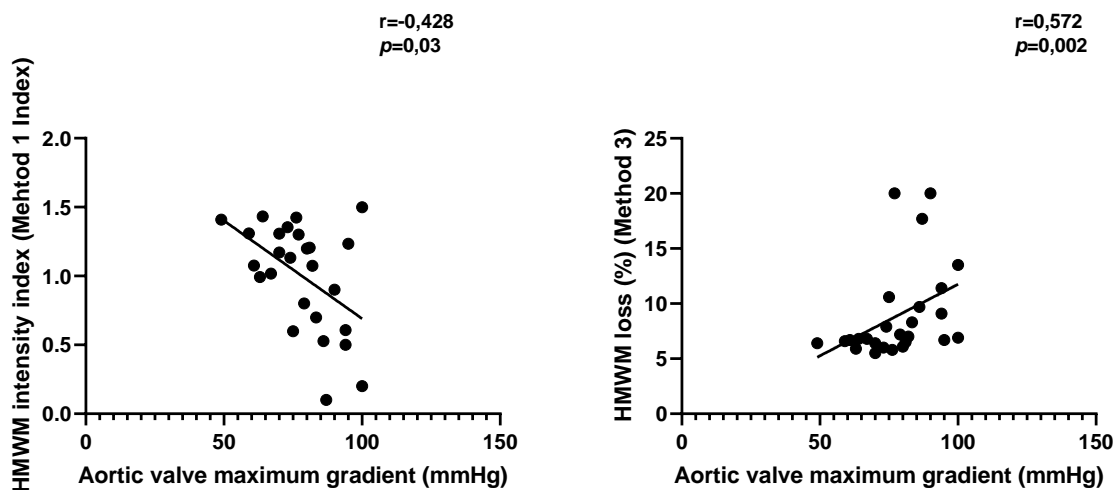


Figure 12. Correlation of vWF multimer pattern with AVS parameters. The vWF HMWM multimer ratio index (left), and loss of HMWM (%) (right) with the aortic valve maximum pressure gradient (mmHg). The lines present in the graphs are regression lines. Each dot represents a patient. Correlation coefficients, and p values are represented at the right top corner of each graph.

Table 9. Spearman correlations between the VWF multimeric profile, as assessed by different methods, and different clinical variables associated with the severity of aortic stenosis before aortic valve replacement. Significant correlations are highlighted.

	Method 1		Method 1 Index		Method 2		Method 2 Index		Method 3		Method 3 Index		vWF Ag U/dl	
	<i>r</i>	<i>p value</i>	<i>r</i>	<i>p value</i>	<i>r</i>	<i>p value</i>	<i>r</i>	<i>p value</i>	<i>r</i>	<i>p value</i>	<i>r</i>	<i>p value</i>	<i>r</i>	<i>p value</i>
<i>AV area (cm²)</i>	-0.063	0.76	0.015	0.94	-0.056	0.79	-0.030	0.89	0.045	0.826	0.023	0.911	-0.065	0.754
<i>Aortic valve maximum gradient</i>	-0.351	0.08	-0.428	0.03	-0.308	0.13	-0.252	0.21	0.572	0.002	0.029	0.888	-0.261	0.198
<i>Mean transvalvular pressure gradient (mmHg)</i>	-0.359	0.05	-0.409	0.02	-0.310	0.10	-0.284	0.13	0.564	0.001	0.267	0.153	-0.107	0.572
<i>Doppler Velocity Index</i>	0.245	0.30	-0.072	0.76	-0.184	0.44	-0.218	0.36	0.144	0.545	-0.189	0.426	0.203	0.390
<i>LV mass</i>	0.161	0.48	0.117	0.60	0.219	0.33	0.128	0.57	0.118	0.600	0.117	0.604	0.032	0.889
<i>LV mass index</i>	0.136	0.55	0.160	0.48	0.234	0.29	0.132	0.56	0.003	0.988	0.107	0.636	-0.045	0.844
<i>LV ejection fraction (%)</i>	-0.191	0.40	-0.356	0.10	-0.387	0.07	-0.339	0.12	0.349	0.111	0.194	0.388	0.033	0.885

Table 10. Postoperative correlations between the VWF multimeric profile as assessed by different methods. and different clinical variables associated with the severity of the disease after valve replacement.

	Method 1		Method 1 Index		Method 2		Method 2 Index		Method 3		Method 3 Index		vWF Ag U/dl	
	<i>r</i>	<i>p value</i>	<i>r</i>	<i>p value</i>	<i>r</i>	<i>p value</i>	<i>r</i>	<i>p value</i>	<i>r</i>	<i>p value</i>	<i>r</i>	<i>p value</i>	<i>r</i>	<i>p value</i>
<i>AV area (cm²)</i>	-0.084	0.794	-0.256	0.420	0.234	0.463	0.139	0.666	0.302	0.337	0.309	0.325	-0.004	1.00
<i>Aortic valve maximum gradient</i>	-0.108	0.724	-0.190	0.531	0.039	0.899	-0.085	0.781	-0.026	0.933	0.113	0.710	-0.061	0.85
<i>Mean transvalvular pressure gradient (mmHg)</i>	-0.160	0.598	-0.133	0.663	-0.040	0.899	-0.047	0.880	-0.151	0.618	-0.004	0.991	0.042	0.894
<i>LV mass</i>	-0.410	0.164	-0.407	0.170	0.020	0.951	0.099	0.750	-0.061	0.845	0.080	0.796	-0.445	0.13
<i>LV mass index</i>	-0.393	0.183	-0.308	0.306	0.003	0.996	0.069	0.825	-0.168	0.580	0.088	0.774	-0.418	0.16
<i>LV ejection fraction (%)</i>	0.508	0.078	0.121	0.692	0.464	0.111	0.239	0.431	-0.039	0.900	-0.338	0.881	0.047	0.88

Differences in vWF HMWM loss before and after aortic valve replacement

To evaluate if the vWF changed after surgery, 13 paired blood samples (supplementary figure 4) were analyzed before and after AVR. No statistical differences were found in the vWF multimer profile (as assessed by any of the three methods previously described) nor in the vWF total antigen levels before, and after the surgery (Figure 13).

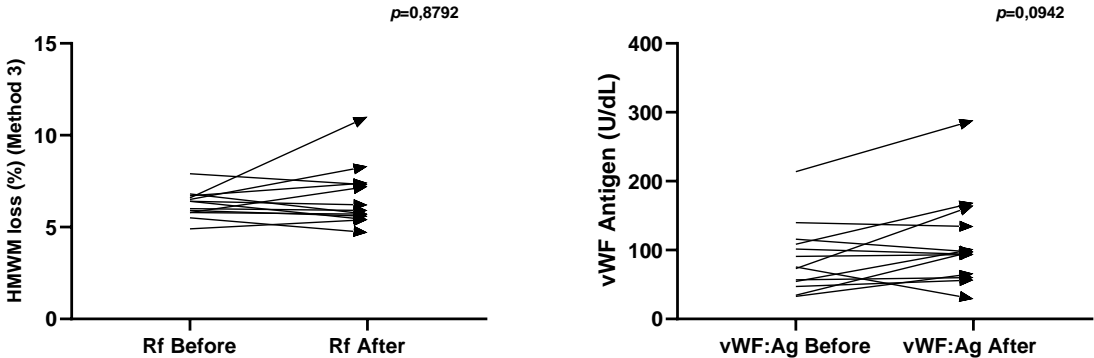


Figure 13. vWF multimer pattern evaluated by the HMWM loss (%) (left) and total vWF antigen (right) in the 13 paired samples before and after aortic valve replacement.

Discussion

The classification of AVS remains an important challenge for physicians, and this affects the diagnosis and prognosis of patients. The connection between the loss of the vWF HMWM, and AVS has long been known and studied previously albeit with contradictory results. In this way, this thesis aim was to study the vWF profile in a cohort of AVS patients. To achieve this the thesis was mainly divided into two main parts. The first part aimed at the optimization of the protocol for vWF multimer analysis including the preparation of PPP, and the implementation of the protocol for the vWF analysis through immuno-electrophoresis. The second part aimed to analyze patients vWF multimer pattern to appraise its value as a biomarker for AVS. This included a comparison between pre- and postoperative timepoints and the identification of potential correlations with clinical variables related to the severity of AVS.

As expected, the PPP centrifugation protocol was optimized quickly however, the same cannot be said of the electrophoresis protocol for the vWF analysis which was constantly beset with technical difficulties.

Regarding the centrifugation protocol to obtain PPP to the best of my knowledge there is currently no standard centrifugation defined in the literature. Still the Clinical and Laboratory Standards Institute recommends that whole blood be centrifuged at 1500 *g* for a minimum of 15 minutes to obtain PPP⁷⁵. All tested conditions created PPP even after just one round of centrifugation. Still, to avoid contamination of platelet-derived vWF a second centrifugation was included in the protocol to assess its efficiency in removing cell fragments present in plasma. Additionally, because platelets can be activated in cold conditions the first centrifugation was done at 18°C. Since the number of platelets was already low after the first centrifugation, and by definition PPP lower temperatures were tested in the second centrifugation to avoid protein degradation.

The best condition was a first centrifugation at 2100 *g* for 15 minutes followed by a second centrifugation at 590 *g* for 15 minutes at 4°C. In the first four tested conditions condition D obtained the lowest density of platelets, probably due to the highest centrifugation speed. This first set of conditions tested was also important to demonstrate that a second centrifugation further reduces platelet numbers although this was not always significant. As for the second centrifugation condition Z (590 *g* for 15 minutes at 4°C) resulted in the lowest and most consistent platelet density. In this second round of tests the duration of centrifugation did not have as much impact on platelet numbers as did temperature. This may be due to the effect of low temperature favoring the precipitation of cells, and other debris, to the bottom of the tube.

A downside of the methodology used is that, firstly, this protocol was optimized in a small number of volunteers, and secondly, no differentiation of platelets from other blood cell types was performed. It is important to emphasize that even with the above stated limitations, the final protocol complied to the definition of PPP. Besides, given that the aim was to obtain a plasma as free as possible of cellular elements the discernability of the said elements is not crucial.

For the vWF electrophoresis, as previously mentioned several detailed protocols already exist^{71,72,76}. However, the adaptation to the PROTEAN® II xi Cell system (Bio-Rad) vertical system proved to be a difficult task and several technical aspects had to be resolved via trial-and-error. Some of the unexpected technical difficulties included, for example, the agarose type to be used, the frequent leaks, the sliding of the agarose gel off of the glass plates, and the difficulties in removing the comb to obtain usable wells. To make the system watertight, thus preventing leaks, an 2% agarose plug was put outside of the system. To prevent the gels from sliding off of the glass plates during the run a 5% polyacrylamide gel with one centimeter height was casted before the agarose gel. To facilitate the removal of the comb the wells depth was fixed one centimeter (exactly 0.7 cm), and the system was refrigerated to 4°C. In the end the comb was removed with extreme care^{71,77}.

Having optimized the protocol to obtain PPP, and the protocol for agarose gel casting the next step was to optimize the immunoelectrophoretic analysis of vWF multimers. In this case, the major difficulty was the normalization of the total vWF densitometric signal. To overcome this problem several strategies were taken including normalization to total protein levels normalization based on the relative amount of vWF, and finally based on the absolute concentration of vWF.

Normalization of vWF to total protein levels has shown to be an inefficient normalization method since it produced an array of different vWF intensities profiles. A second attempt was based on relative quantification of vWF by slot blot using the same antibody as for immune electrophoresis. Even when normalized via slot blot to a reference sample with a well-defined vWF multimer pattern the optical density was irregular with some samples showing overlapping or indistinguishable bands while other samples presented barely noticeable vWF multimers. This is explained by an over or underestimation of vWF quantities. Usually, this discrepancy occurred in plasma samples where the total protein quantities, and vWF signal were at extremes, for example, in samples where there was a lot of total protein but a weak vWF signal (when compared to a reference sample), and vice versa. To my knowledge this strategy has not been previously attempted hence, no comparisons can be made with previous studies.

With regard to the performance of absolute quantification for sample normalization it worked better than vWF relative quantification with only slight differences in OD that did not affect sample analysis. This could be due to several factors inherent to the slot blot technique. Including, the lack of known vWF protein standards, and artifacts that interfere with OD such as membrane background. Absolute quantification of vWF was performed via ELISA which is a more sensitive, and specific quantification technique when compared to quantification via slot blot.

Another major issue to tackle on vWF analysis is the need for a robust and sensible method for multimer analysis that can be translated to clinical practice. Different approaches have been proposed^{73,74} and attempted in this thesis. All methods have advantages and disadvantages. Starting with method 1 which evaluated the multimer pattern via peak intensities. This method and its index correlated the worst with parameters of AVS severity. This may be in part due to inherent limitations of vWF electrophoresis. In some gels, due to artifacts, the low and intermediate MWM were fainter than the HMWM. This may have skewed method 1 results, which in turn would result in worse correlations with AVS parameters. As for method 3 which measures HMWM loss (%), and it is not dependent on pixel intensity correlations were greater and more significant. Additionally, merely by measuring the loss of the multimers this method does not rely on a previously established, and arbitrary cut off for the HMWM. Indeed, the definition of HMWM has been arbitrary with some authors defining HMWM any multimer above band 10⁶⁴, others band 11 or even band 15⁶⁸. Several attempts to overcome this problem were made using an unstained protein ladder of hyaluronic acid with a high molecular weight (2 to 8 Megadalton). However, an adequate ladder staining on the gel was not obtained. Overall, these factors explain the higher performance of Method 3 compared to Method 1 and Method 2.

The correlation between the vWF multimer pattern, and parameters of AVS severity namely mean transvalvular pressure gradient, peak velocity, and aortic valve area have been previously reported elsewhere^{65,68-70,74}. This study in part corroborates these results by finding a correlation with the mean and maximum pressure gradients. Indeed, as disease progresses the aortic valve area decreases due to the fibrosis and calcification of the valve, and consequently, the pressure gradients increase. In most cases this also results in LV hypertrophy since there is an increase in the pressure that the LV must exert to pump blood. Additionally, with the increase in shear stress the degradation of the vWF factor increases⁶⁶. Unsurprisingly, when evaluating the multimer pattern via peak intensities (Method 1), and its index negative correlations were found with mean, and maximum pressure gradients. Since this method measures the amount of HMWM present in a sample, the lower the ratio, the less

HMWM is present so, the higher the vWF degradation. On the other hand, method 3 is a direct measure of the HMWM loss hence, it correlates positively with the mean and maximum pressure gradients.

Associations between vWF multimer profile, and LV measurements such as LV mass, mass index, and ejection fraction were investigated since LV hypertrophy which occurs with AVS, is a marker of poor prognosis. No significant correlation was found between LV measurements, and vWF multimer pattern. Unsurprisingly, there was no correlation between the vWF multimer pattern and the ejection fraction. The preserved ejection fraction of the study population supports this.

Contrary to other reports⁶⁸, it was unable to find a correlation between the aortic valve area, and the vWF multimer profile. In part, this may be explained by the use of different methods to quantify HMWM loss or the lower number of patients used in this study.

Focusing on the paired samples, no differences were found between the vWF multimer pattern or antigen levels. In part, this can be explained by the low number of paired samples, and because in our cohort vWF HMWM loss was not as high as it would be expected. Only 5 (17%) patient's samples had a visual loss of the HMWM in the gel. Most had a normal multimeric pattern many times indistinguishable from the control (Supplementary figure 4). In other studies, the loss of the HMWM can vary between 42%⁶⁵, 57%⁶⁸ to 80%⁶⁹. This discrepancy may explain why the vWF multimer pattern showed no statistical difference in the paired analysis.

When considering only the postoperative samples, no correlations were found between the vWF multimer pattern, and AVS severity parameters. This can be explained simply by the successful valve replacement, and by the fact that none of the patients had paravalvular regurgitation.

The possible effect of medication and vWF parameters was also investigated since several drugs have been described to cause AvWS. Indeed, certain medications decrease vWF synthesis (valproic acid) or enhance its proteolysis (ciprofloxacin)⁷⁸. However, to my knowledge no information on the impact of the different drug classes analyzed in this study, and AvWS is available in the literature. Regardless, no differences were observed in the vWF multimer pattern or antigen between patients that took medication *versus* those that did not.

This study has its limitations. First, being a retrospective study, some data was missing in some of the tested variables reducing its statistical power. This together with the lack of data regarding bleeding history other vWF indexes like vWF:RCo, and other biochemical parameters made it impossible to further characterize the AvWS. In addition to this none of the

patients studied presented paravalvular leak which precluded the analysis of the biomarker value of vWF multimer for this specific complication.

Conclusions

The fundamental finding of this thesis is that the echocardiographic measures used to evaluate the severity of AVS correlate with the vWF multimer pattern.

Regarding the protocol to obtain PPP one centrifugation step is enough to obtain PPP but a second centrifugation further reduces cell fragment numbers. The ideal condition involves two consecutive centrifugations: one at 2100 *g* for 15 minutes at 18°C followed by other at 590 *g* for 15 minutes at 4 °C.

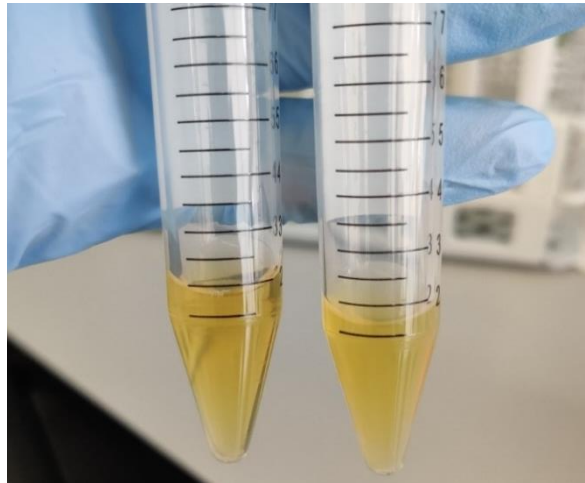
Regarding the measurement of vWF absolute quantification is required to analyze vWF multimer pattern since relative quantification does not produce a comparable multimer pattern. The examination of the HMWM loss (%) by method 3 turned out to be the optimum method for evaluating such a pattern.

Additionally, this thesis further corroborates the vWF potential as a biomarker of AVS since the vWF multimeric pattern correlated with the mean and maximum pressure gradients. Still, no correlation was found between LV parameters and the vWF multimer profile.

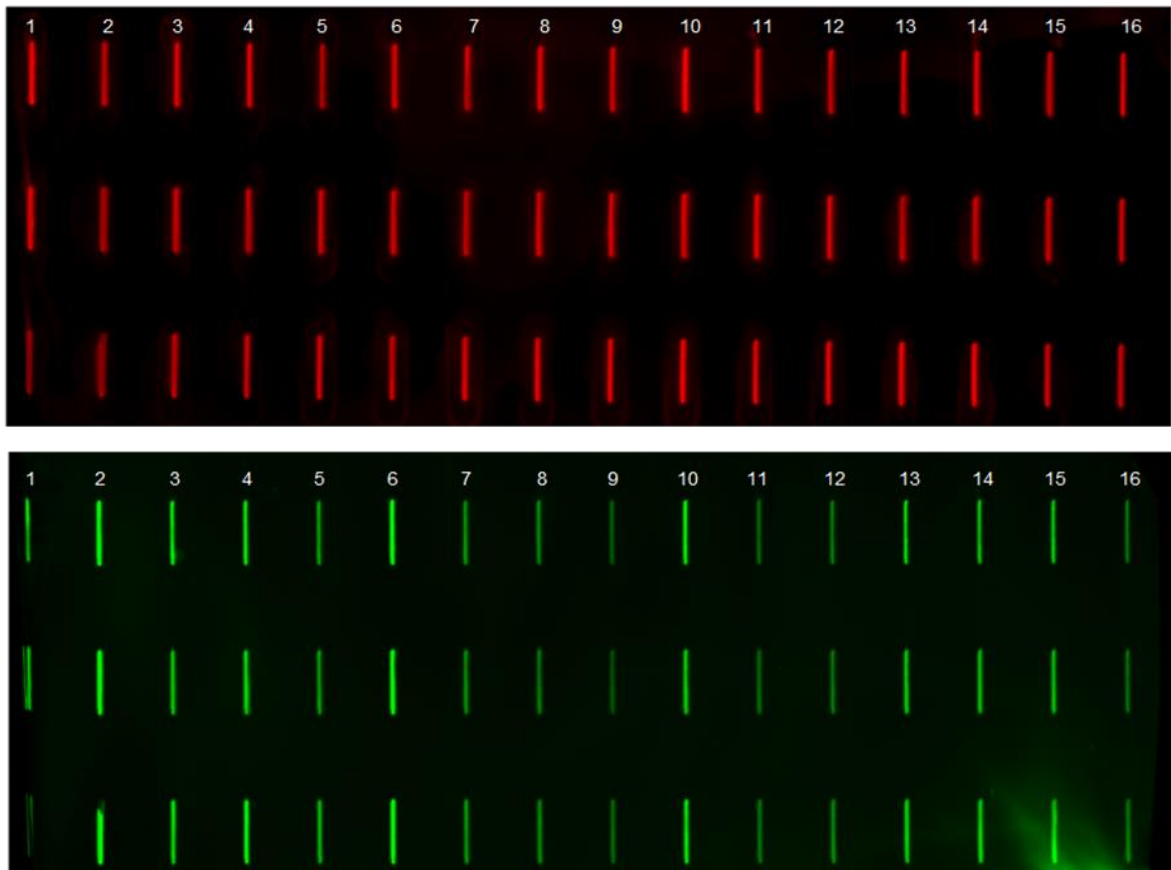
In the paired analysis, there was no correlation between the multimeric pattern of vWF, and AVS severity measurements. The same is true when considering the postoperative samples.

Despite being a small study, the optimizations performed, and the pilot data obtained will help guide future studies namely in terms of methods used to evaluate the vWF, contributing to a general standardization of the protocols used. Still, further optimization of the technique for the visualization of the vWF multimers is needed to become a routine procedure. Even though several studies have already evaluated the vWF multimer pattern in patients with AVS, multicenter studies are lacking. In order to fill this gap, this work is part of a research project that is being carried out in both CHUSJ, and Centro Hospitalar de Vila Nova de Gaia to study the vWF multimer pattern in AVS patients.

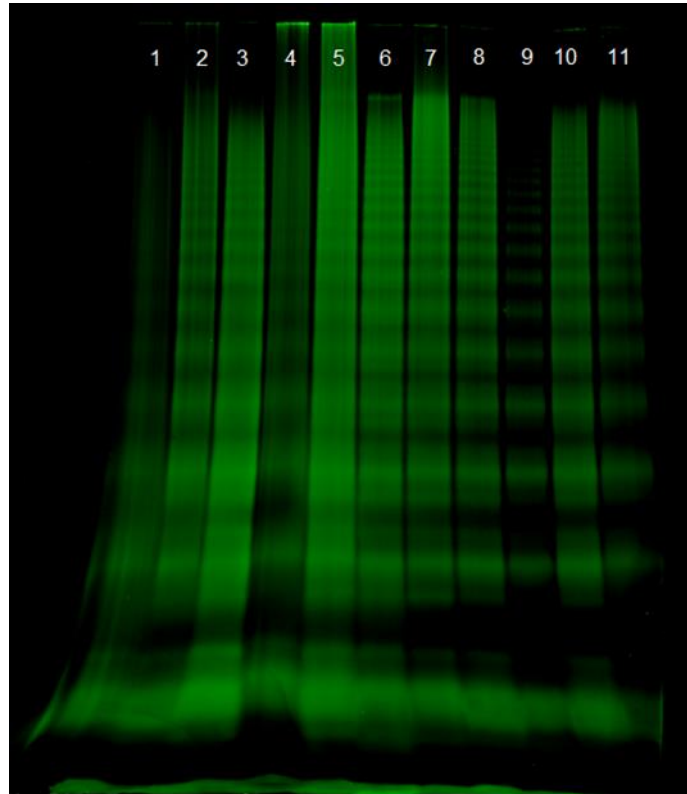
Supplements



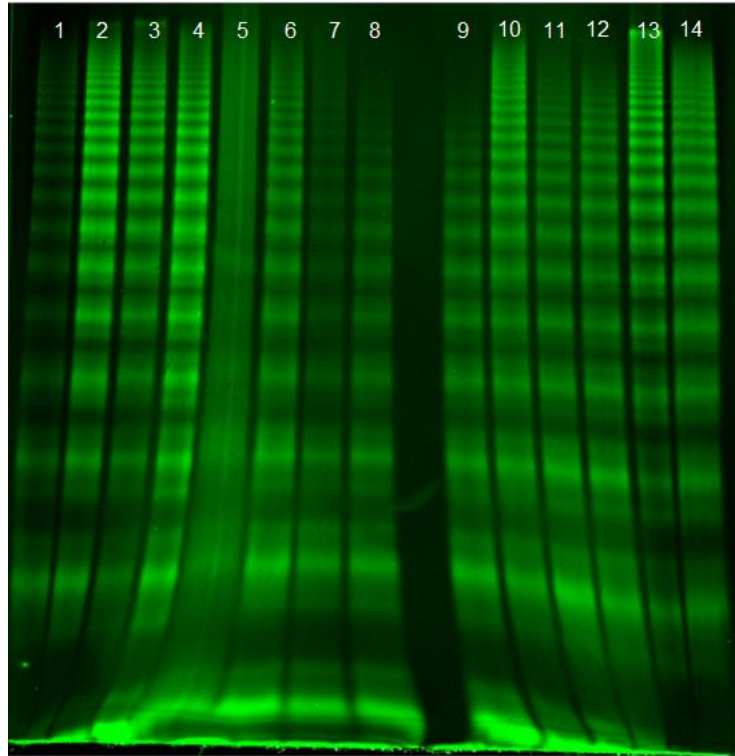
Supplementary figure 1. Plasma of a healthy volunteer when submitted to different test conditions for PPP obtention. On the left plasma that was submitted to 150 g for 10 minutes (test condition C), and on the right 2100 g for 15 minutes (test condition D).



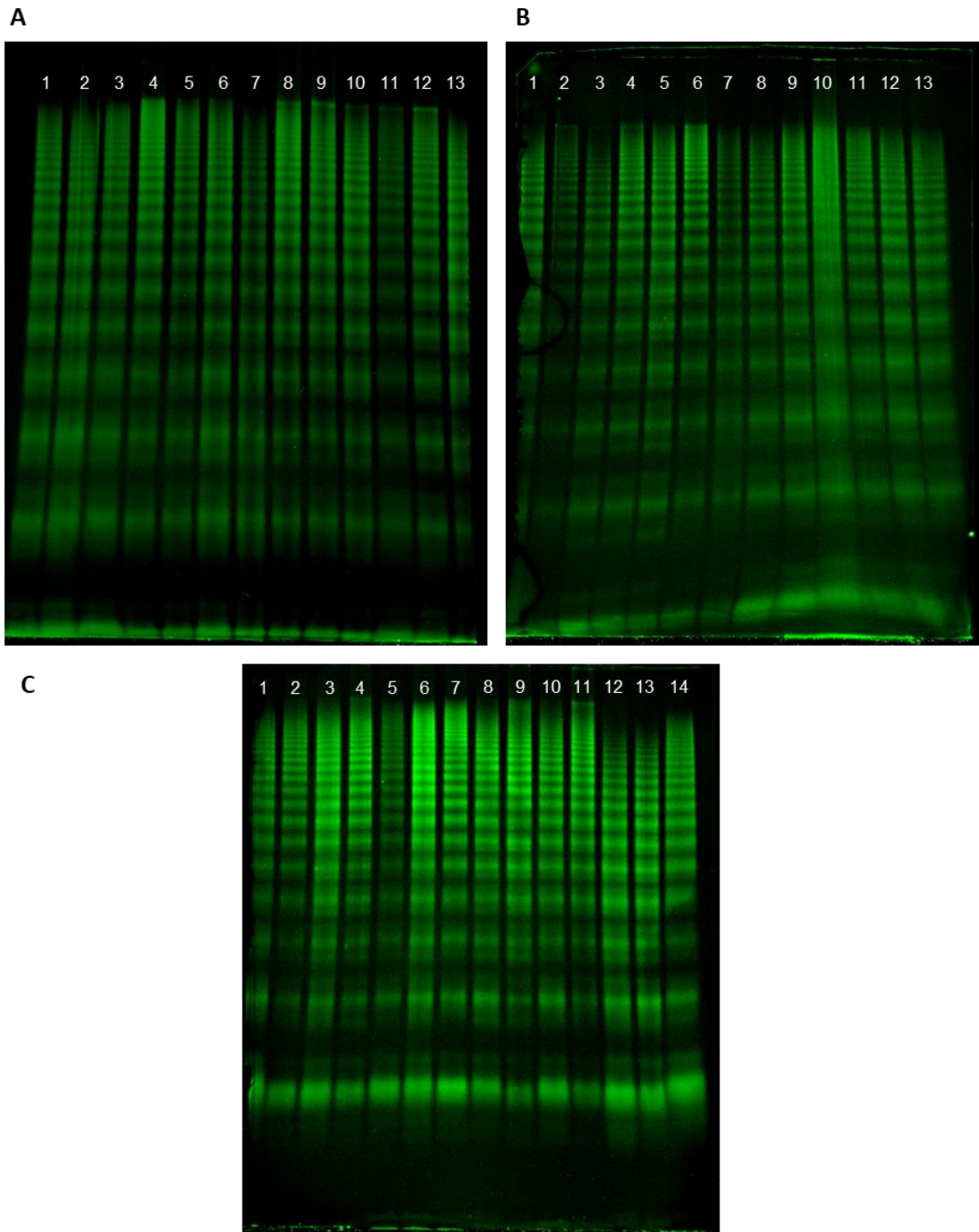
Supplementary figure 2. Slot blot membrane with total protein staining (top) and vWF (bottom). Samples 1 to 15 are from patients with AVS, while samples 15 and 16 are from healthy volunteers. Samples are triplicated vertically. The reference sample is in lane 2.



Supplementary figure 3. Agarose gel of vWF normalized via relative quantification. Samples 1 through 8 are from patients with AVS, and samples 9 through 11 are samples from healthy volunteers. Sample 3, 4 and 5 correspond to sample 1, 2 and 3 in Figure 10, in the results section. Samples 10, and 11 correspond to samples from healthy volunteers 4 and 5 respectively in Figure 10.



Supplementary figure 4. Agarose gel of vWF normalized via absolute quantification. Samples 1 through 14 are samples from patients with AVS. Sample 14 is from a healthy volunteer. Sample 5 was excluded from the analysis due to the inability of extracting the vWF multimer pattern.



Supplementary figure 5. Agarose gel of vWF normalized via absolute quantification. In gel A, healthy volunteers are in lanes 1,2 and 3 while in gel B, healthy volunteers are in lanes 11, 12 and 13. Lastly, in gel C only one sample of a healthy volunteer was placed in lane 14. In gel A preoperative samples are in lanes: 9, 10, 11, 12, 13, and are paired with postoperative samples in lanes: 8, 6, 4, 5, 7 respectively. In gel B preoperative samples are in lanes: 1, 2, 3, 4, 5 and are paired with postoperative samples in lanes: 7, 6, 8, 9, 10 respectively. Samples 1 in gel B was reloaded in gel C in lane 1. Lastly in gel C preoperative samples are in lanes: 2, 3, 4 and are paired with postoperative samples in lanes: 7, 6, 5 respectively. Lanes 8 through 11 are from preoperative samples.

Supplementary table 1. Solutions used for the analysis of vWF multimers.

Solutions	Composition
Antibody buffer solution	5% BSA in TBS-Tween 0.05%
Electrode buffer (Stable for at least 1 month at 4 °C)	50 mM Tris. 384 mM glycine and 0.1% (w/v) SDS, 5 mM/L Na ₂ EDTA; pH 8.3 (not adjusted)
Fixing solution	50% Isopropanol 5% Acetic Acid
Running gel buffer (Stable for at least 1 month at 4 °C)	0.1 M Tris. 0.1 M glycine. and 0.4% (w/v) SDS 5 mM/L Na ₂ EDTA; pH 8.8
Running gel (Stable for 4 h)	2% (w/v) of high gelling temperature agarose in running gel buffer
Sample buffer (Stable for at least 6 months at 4 °C)	10 mM Tris. 1 mM Na ₂ EDTA. 2% SDS. 20% glycerol. and 2 mg/mL bromophenol blue (pH was not adjusted)
Stacking gel buffer (Stable for at least 1 month at 4 °C)	70 mM Tris. 4 mM Na ₂ EDTA. and 0.4% (w/v) SDS. pH 6.8
Stacking gel (Stable for 4 h)	0.8% (w/v) of high gelling temperature agarose in stacking gel buffer
Tris buffer saline	50 Mm Tris, 150 mM NaCl pH 7.5
Washing Solution	TBS-Tween 0.05%

Abbreviations; BSA. Bovine Serum Albumin; TBS. Tris Buffer Saline; SDS. Sodium dodecyl sulfate; (w/v); weight/volume

References

1. O'Brien, K.D. Epidemiology and genetics of calcific aortic valve disease. *J Investig Med* 55, 284-291 (2007),10.2310/6650.2007.00010.
2. Alushi, B., et al. Calcific Aortic Valve Disease-Natural History and Future Therapeutic Strategies. *Front Pharmacol* 11, 685 (2020),10.3389/fphar.2020.00685.
3. Stewart, B.F., et al. Clinical factors associated with calcific aortic valve disease. Cardiovascular Health Study. *J Am Coll Cardiol* 29, 630-634 (1997),10.1016/s0735-1097(96)00563-3.
4. Goody, P.R., et al. Aortic Valve Stenosis: From Basic Mechanisms to Novel Therapeutic Targets. *Arterioscler Thromb Vasc Biol* 40, 885-900 (2020),10.1161/ATVBAHA.119.313067.
5. Bartoli-Leonard, F., Zimmer, J. & Aikawa, E. Innate and adaptive immunity: the understudied driving force of heart valve disease. *Cardiovascular Research* 117, 2506-2524 (2021),10.1093/cvr/cvab273.
6. Kazik, H.B., Kandail, H.S., LaDisa, J.F., Jr. & Lincoln, J. Molecular and Mechanical Mechanisms of Calcification Pathology Induced by Bicuspid Aortic Valve Abnormalities. *Frontiers in cardiovascular medicine* 8, 677977-677977 (2021),10.3389/fcvm.2021.677977.
7. Cuevas, R.A., et al. Isolation of Human Primary Valve Cells for In vitro Disease Modeling. *J Vis Exp* (2021),10.3791/62439.
8. Dweck, M.R., Boon, N.A. & Newby, D.E. Calcific Aortic Stenosis: A Disease of the Valve and the Myocardium. *Journal of the American College of Cardiology* 60, 1854-1863 (2012),<https://doi.org/10.1016/j.jacc.2012.02.093>.
9. Akahori, H., Tsujino, T., Masuyama, T. & Ishihara, M. Mechanisms of aortic stenosis. *Journal of Cardiology* 71, 215-220 (2018),doi.org/10.1016/j.jjcc.2017.11.007.
10. Liu, A.C., Joag, V.R. & Gotlieb, A.I. The emerging role of valve interstitial cell phenotypes in regulating heart valve pathobiology. *Am J Pathol* 171, 1407-1418 (2007),10.2353/ajpath.2007.070251.
11. Pawade, T.A., Newby, D.E. & Dweck, M.R. Calcification in Aortic Stenosis: The Skeleton Key. *Journal of the American College of Cardiology* 66, 561-577 (2015),<https://doi.org/10.1016/j.jacc.2015.05.066>.
12. Cowell, S.J., et al. A randomized trial of intensive lipid-lowering therapy in calcific aortic stenosis. *N Engl J Med* 352, 2389-2397 (2005),10.1056/NEJMoa043876.
13. Novaro, G.M., et al. Effect of hydroxymethylglutaryl coenzyme a reductase inhibitors on the progression of calcific aortic stenosis. *Circulation* 104, 2205-2209 (2001),10.1161/hc4301.098249.
14. Shavelle, D.M., et al. HMG CoA reductase inhibitor (statin) and aortic valve calcium. *The Lancet* 359, 1125-1126 (2002),[doi.org/10.1016/S0140-6736\(02\)08161-8](https://doi.org/10.1016/S0140-6736(02)08161-8).
15. Rosenhek, R., et al. Statins but Not Angiotensin-Converting Enzyme Inhibitors Delay Progression of Aortic Stenosis. *Circulation* 110, 1291-1295 (2004),[doi:10.1161/01.CIR.0000140723.15274.53](https://doi.org/10.1161/01.CIR.0000140723.15274.53).
16. Moura, L.M., et al. Rosuvastatin Affecting Aortic Valve Endothelium to Slow the Progression of Aortic Stenosis. *Journal of the American College of Cardiology* 49, 554-561 (2007),doi.org/10.1016/j.jacc.2006.07.072.

17. Rossebø, A.B., *et al.* Intensive lipid lowering with simvastatin and ezetimibe in aortic stenosis. *N Engl J Med* 359, 1343-1356 (2008),10.1056/NEJMoa0804602.
18. Chan, K.L., Teo, K., Dumesnil, J.G., Ni, A. & Tam, J. Effect of Lipid Lowering With Rosuvastatin on Progression of Aortic Stenosis. *Circulation* 121, 306-314 (2010),doi:10.1161/CIRCULATIONAHA.109.900027.
19. Hermans, H., *et al.* Statins for Calcific Aortic Valve Stenosis: Into Oblivion After SALTIRE and SEAS? An Extensive Review from Bench to Bedside. *Current Problems in Cardiology* 35, 284-306 (2010),doi.org/10.1016/j.cpcardiol.2010.02.002.
20. Pawade, T.A., *et al.* Effect of Denosumab or Alendronic Acid on the Progression of Aortic Stenosis: A Double-Blind Randomized Controlled Trial. *Circulation* 143, 2418-2427 (2021),10.1161/CIRCULATIONAHA.121.053708.
21. Demer, L.L. & Tintut, Y. Hearts of Stone: Calcific Aortic Stenosis and Antiresorptive Agents for Osteoporosis. *Circulation* 143, 2428-2430 (2021),10.1161/CIRCULATIONAHA.121.054823.
22. Natorska, J., Kopytek, M. & Undas, A. Aortic valvular stenosis: Novel therapeutic strategies. *Eur J Clin Invest* 51, e13527 (2021),10.1111/eci.13527.
23. Lindman, B.R., *et al.* Calcific aortic stenosis. *Nature Reviews Disease Primers* 2, 16006 (2016),10.1038/nrdp.2016.6.
24. Baumgartner, H., *et al.* Echocardiographic assessment of valve stenosis: EAE/ASE recommendations for clinical practice. *European Journal of Echocardiography* 10, 1-25 (2009),10.1093/ejechocard/jen303.
25. Vahanian, A., *et al.* 2021 ESC/EACTS Guidelines for the management of valvular heart disease. *Eur Heart J* 43, 561-632 (2022),10.1093/eurheartj/ehab395.
26. Guzzetti, E., Annabi, M.S., Pibarot, P. & Clavel, M.A. Multimodality Imaging for Discordant Low-Gradient Aortic Stenosis: Assessing the Valve and the Myocardium. *Front Cardiovasc Med* 7, 570689 (2020),10.3389/fcvm.2020.570689.
27. Messika-Zeitoun, D. & Lloyd, G. Aortic valve stenosis: evaluation and management of patients with discordant grading. *E-journal Cardiol Pract* 15, 26 (2018)
28. Harris, A.W., Pibarot, P. & Otto, C.M. Aortic Stenosis: Guidelines and Evidence Gaps. *Cardiol Clin* 38, 55-63 (2020),10.1016/j.ccl.2019.09.003.
29. Ito, S., Miranda, W.R., Jaffe, A.S. & Oh, J.K. Prognostic Value of N-Terminal Pro-form B-Type Natriuretic Peptide in Patients With Moderate Aortic Stenosis. *Am J Cardiol* 125, 1566-1570 (2020),10.1016/j.amjcard.2020.02.004.
30. Darren, M., Haytham, M. & Nicolo, P. Paravalvular aortic regurgitation after TAVI: new insight. *EuroIntervention* 11, 371-372 (2015)
31. Yasar, S.J., Abdullah, O., Fay, W. & Balla, S. Von Willebrand factor revisited. *Journal of Interventional Cardiology* 31, 360-367 (2018),doi.org/10.1111/joic.12478.
32. Leebeek, F.W. & Eikenboom, J.C. Von Willebrand's Disease. *N Engl J Med* 375, 2067-2080 (2016),10.1056/NEJMra1601561.
33. Sadler, J.E. BIOCHEMISTRY AND GENETICS OF VON WILLEBRAND FACTOR. *Annual Review of Biochemistry* 67, 395-424 (1998),10.1146/annurev.biochem.67.1.395.
34. Nilsson, I.M. The history of von Willebrand disease. *Haemophilia* 5, 7-11 (1999),doi.org/10.1046/j.1365-2516.1999.0050s2007.x.

35. Swami, A. & Kaur, V. von Willebrand Disease: A Concise Review and Update for the Practicing Physician. *Clinical and Applied Thrombosis/Hemostasis* 23, 900-910 (2016),10.1177/1076029616675969.
36. James, P.D., *et al.* ASH ISTH NHF WFH 2021 guidelines on the diagnosis of von Willebrand disease. *Blood Advances* 5, 280-300 (2021),10.1182/bloodadvances.2020003265.
37. de Jong, A. & Eikenboom, J. Von Willebrand disease mutation spectrum and associated mutation mechanisms. *Thrombosis Research* 159, 65-75 (2017),doi.org/10.1016/j.thromres.2017.09.025.
38. Tiede, A. Diagnosis and treatment of acquired von Willebrand syndrome. *Thrombosis Research* 130, S2-S6 (2012),10.1016/s0049-3848(13)70003-3.
39. TIEDE, A., *et al.* Diagnostic workup of patients with acquired von Willebrand syndrome: a retrospective single-centre cohort study. *Journal of Thrombosis and Haemostasis* 6, 569-576 (2008),doi.org/10.1111/j.1538-7836.2008.02909.x.
40. Casonato, A., *et al.* von Willebrand factor abnormalities in aortic valve stenosis: Pathophysiology and impact on bleeding. *Thrombosis and haemostasis* 106, 58-66 (2011),10.1160/TH10-10-0634.
41. Denis, C.V. Molecular and cellular biology of von Willebrand factor. *Int J Hematol* 75, 3-8 (2002),10.1007/bf02981972.
42. Stocksclaeder, M., Schneppenheim, R. & Budde, U. Update on von Willebrand factor multimers: focus on high-molecular-weight multimers and their role in hemostasis. *Blood coagulation & fibrinolysis : an international journal in haemostasis and thrombosis* 25, 206-216 (2014),10.1097/MBC.000000000000065.
43. Lenting, P.J., Christophe, O.D. & Denis, C.V. von Willebrand factor biosynthesis, secretion, and clearance: connecting the far ends. *Blood* 125, 2019-2028 (2015),10.1182/blood-2014-06-528406.
44. Ward, S., O'Sullivan, J.M. & O'Donnell, J.S. von Willebrand factor sialylation-A critical regulator of biological function. *J Thromb Haemost* 17, 1018-1029 (2019),10.1111/jth.14471.
45. Springer, T.A. von Willebrand factor, Jedi knight of the bloodstream. *Blood* 124, 1412-1425 (2014),10.1182/blood-2014-05-378638.
46. Ledford-Kraemer, M.R. Analysis of von Willebrand factor structure by multimer analysis. *Am J Hematol* 85, 510-514 (2010),10.1002/ajh.21739.
47. Okhota, S., Melnikov, I., Avtaeva, Y., Kozlov, S. & Gabbasov, Z. Shear Stress-Induced Activation of von Willebrand Factor and Cardiovascular Pathology. *Int J Mol Sci* 21(2020),10.3390/ijms21207804.
48. Ishihara, J., *et al.* The heparin binding domain of von Willebrand factor binds to growth factors and promotes angiogenesis in wound healing. *Blood* 133, 2559-2569 (2019),10.1182/blood.2019000510.
49. Giblin, J.P., Hewlett, L.J. & Hannah, M.J. Basal secretion of von Willebrand factor from human endothelial cells. *Blood* 112, 957-964 (2008),doi.org/10.1182/blood-2007-12-130740.
50. Kawecky, C., Lenting, P.J. & Denis, C.V. von Willebrand factor and inflammation. *J Thromb Haemost* 15, 1285-1294 (2017),10.1111/jth.13696.

51. Pimanda, J.E., *et al.* Role of Thrombospondin-1 in Control of von Willebrand Factor Multimer Size in Mice*. *Journal of Biological Chemistry* 279, 21439-21448 (2004),doi.org/10.1074/jbc.M313560200.
52. Federici, A.B., *et al.* Binding of von Willebrand factor to glycoproteins Ib and IIb/IIIa complex: affinity is related to multimeric size. *Br J Haematol* 73, 93-99 (1989),10.1111/j.1365-2141.1989.tb00226.x.
53. Feng, Y., *et al.* ADAMTS13: more than a regulator of thrombosis. *Int J Hematol* 104, 534-539 (2016),10.1007/s12185-016-2091-2.
54. Arya, M., *et al.* Ultralarge multimers of von Willebrand factor form spontaneous high-strength bonds with the platelet glycoprotein Ib-IX complex: studies using optical tweezers. *Blood* 99, 3971-3977 (2002),doi.org/10.1182/blood-2001-11-0060.
55. Sarig, G. ADAMTS-13 in the Diagnosis and Management of Thrombotic Microangiopathies. *Rambam Maimonides Med J* 5, e0026-e0026 (2014),10.5041/RMMJ.10160.
56. De Ceunynck, K., De Meyer, S.F. & Vanhoorelbeke, K. Unwinding the von Willebrand factor strings puzzle. *Blood* 121, 270-277 (2013),10.1182/blood-2012-07-442285.
57. Dong, J.F., *et al.* ADAMTS-13 rapidly cleaves newly secreted ultralarge von Willebrand factor multimers on the endothelial surface under flowing conditions. *Blood* 100, 4033-4039 (2002),10.1182/blood-2002-05-1401.
58. Hubeau, C., Rocks, N. & Cataldo, D. ADAM28: Another ambivalent protease in cancer. *Cancer Letters* 494, 18-26 (2020),doi.org/10.1016/j.canlet.2020.08.031.
59. Albáñez, S., *et al.* Aging and ABO blood type influence von Willebrand factor and factor VIII levels through interrelated mechanisms. *Journal of Thrombosis and Haemostasis* 14, 953-963 (2016),doi.org/10.1111/jth.13294.
60. Mojzisch, A. & Brehm, M.A. The Manifold Cellular Functions of von Willebrand Factor. *Cells* 10(2021),10.3390/cells10092351.
61. Patmore, S., Dhimi, S.P.S. & O'Sullivan, J.M. Von Willebrand factor and cancer; metastasis and coagulopathies. *Journal of Thrombosis and Haemostasis* 18, 2444-2456 (2020),doi.org/10.1111/jth.14976.
62. Selvam, S. & James, P. Angiodysplasia in von Willebrand Disease: Understanding the Clinical and Basic Science. *Semin Thromb Hemost* 43, 572-580 (2017),10.1055/s-0037-1599145.
63. Randi, A.M. & Laffan, M.A. Von Willebrand factor and angiogenesis: basic and applied issues. *J Thromb Haemost* 15, 13-20 (2017),10.1111/jth.13551.
64. Sedaghat, A., *et al.* Transcatheter aortic valve implantation leads to a restoration of von Willebrand factor (VWF) abnormalities in patients with severe aortic stenosis - Incidence and relevance of clinical and subclinical VWF dysfunction in patients undergoing transfemoral TAVI. *Thromb Res* 151, 23-28 (2017),10.1016/j.thromres.2016.12.027.
65. Spangenberg, T., *et al.* Treatment of Acquired von Willebrand Syndrome in Aortic Stenosis With Transcatheter Aortic Valve Replacement. *JACC: Cardiovascular Interventions* 8, 692-700 (2015),doi.org/10.1016/j.jcin.2015.02.008.
66. Van Belle, E., *et al.* von Willebrand Factor and Management of Heart Valve Disease: JACC Review Topic of the Week. *J Am Coll Cardiol* 73, 1078-1088 (2019),10.1016/j.jacc.2018.12.045.

67. Van Belle, E., *et al.* Von Willebrand Factor Multimers during Transcatheter Aortic-Valve Replacement. *New England Journal of Medicine* 375, 335-344 (2016),10.1056/NEJMoa1505643.
68. Blackshear, J.L., *et al.* Indexes of von Willebrand factor as biomarkers of aortic stenosis severity (from the Biomarkers of Aortic Stenosis Severity [BASS] study). *Am J Cardiol* 111, 374-381 (2013),10.1016/j.amjcard.2012.10.015.
69. Vincentelli, A., *et al.* Acquired von Willebrand Syndrome in Aortic Stenosis. *New England Journal of Medicine* 349, 343-349 (2003),10.1056/NEJMoa022831.
70. Frank, R.D., Lanzmich, R., Haager, P.K. & Budde, U. Severe Aortic Valve Stenosis:Sustained Cure of Acquired von Willebrand Syndrome After Surgical Valve Replacement. *Clinical and Applied Thrombosis/Hemostasis* 23, 229-234 (2017),10.1177/1076029616660759.
71. Thomazini, C.M., Soares, R.P.S., da Rocha, T.R.F., Sachetto, A.T.A. & Santoro, M.L. Optimization of von Willebrand factor multimer analysis in vertical mini-gel electrophoresis systems: A rapid procedure. *Thromb Res* 175, 76-83 (2019),10.1016/j.thromres.2019.01.018.
72. Pruthi, R.K., *et al.* Plasma von Willebrand factor multimer quantitative analysis by in-gel immunostaining and infrared fluorescent imaging. *Thromb Res* 126, 543-549 (2010),10.1016/j.thromres.2010.09.015.
73. Hennessy-Strahs, S., Bermudez, C.A., Acker, M.A. & Bartoli, C.R. Toward a Standard Practice to Quantify von Willebrand Factor Degradation During Left Ventricular Assist Device Support. *The Annals of Thoracic Surgery* 112, 1257-1264 (2021),doi.org/10.1016/j.athoracsur.2020.09.039.
74. Tamura, T., *et al.* Unexpectedly High Prevalence of Acquired von Willebrand Syndrome in Patients with Severe Aortic Stenosis as Evaluated with a Novel Large Multimer Index. *J Atheroscler Thromb* 22, 1115-1123 (2015),10.5551/jat.30809.
75. Favaloro, E.J. & Lippi, G. *Hemostasis and thrombosis methods and protocols*, (Humana Press, New York, 2017).
76. Ott, H.W., *et al.* Analysis of von Willebrand factor multimers by simultaneous high- and low-resolution vertical SDS-agarose gel electrophoresis and Cy5-labeled antibody high-sensitivity fluorescence detection. *Am J Clin Pathol* 133, 322-330 (2010),10.1309/AJCPZSBTD2BWOMVL.
77. Warren, C.M., Krzesinski, P.R. & Greaser, M.L. Vertical agarose gel electrophoresis and electroblotting of high-molecular-weight proteins. *Electrophoresis* 24, 1695-1702 (2003),10.1002/elps.200305392.
78. Mital, A. Acquired von Willebrand Syndrome. *Adv Clin Exp Med* 25, 1337-1344 (2016),10.17219/acem/64942.